

ESA-TR-71-01

January 1971

AD 888 503 L

BETA - RADIATION DOSES
FROM FALLOUT PARTICLES
DEPOSITED ON THE SKIN


Environmental

Science

Associates

Distribution limited to U.S. Govern-
ment Agencies only; ~~cannot be released~~
~~for public release. Do not cite as~~
~~find reference.~~ Other requests for
this document must be referred to
OSA, Office of Civil Defense, Re-
search. Wash DC 20310

Final Report
Contract No DAHC20-70-C-0289
OCD Work Unit No 3117G



ESA-TR-71-01

BETA -RADIATION DOSES FROM FALLOUT
PARTICLES DEPOSITED ON THE SKIN

For
The Office of Civil Defense
Department of the Army

Contract No. DAHC20-70-C-0289

by

S. Z. Mikhail

January 1971

Environmental Science Associates
770 Airport Boulevard
Burlingame, California 94010

BETA-RADIATION DOSES FROM FALLOUT
PARTICLES DEPOSITED ON THE SKIN

SUMMARY

Final Report

For

The Office of Civil Defense

Department of the Army

Contract No. DAHC20-70-C-0289

by

S. Z. Mikhail

January 1971

Environmental Science Associates
770 Airport Boulevard
Burlingame, California 94010

SUMMARY

A. Objectives

1. To estimate (compute) the beta-dose delivery to human skin from land-surface-burst fallout particles, individually and collectively deposited on the skin.
2. To compare the computed beta doses with established skin-damage criteria; from this, to determine conditions under which damage to the skin is expected.
3. To investigate the effect of radionuclide fractionation of fission-product inventory on beta-dose delivery.
4. To carry out sample calculations of gamma-dose delivery to the skin from the same particulate-fallout sources.

B. Assumptions

1. The mechanism of fission-product absorption in fallout-particle material is diffusion controlled.
2. Radioactive fallout contains 10^{15} equivalent fissions per cubic centimeter.
3. Particle-size distribution in fallout is log-normal.
4. Formation of a skin lesion one millimeter in diameter constitutes the threshold for local damage to the skin.

C. Findings

1. By use of the Beta Transmission, Degradation and Dissipation Model, expected beta doses from single fallout particles

C. Findings (Continued)

were estimated for parametric values of (a) particle size, (b) skin-exposure periods and (c) time delays between detonation and deposition on the skin.

2. No single particle is expected to cause skin damage if fallout deposits on the skin later than three hours post-detonation.

3. Fractionation causes a decrease in dose delivery by as much as a factor of two.

4. Gamma dose constitutes only a small fraction of the total dose delivery from smaller particles. The gamma-to-beta dose ratio increases with particle size.

5. Estimates of expected doses from multiparticle fallout deposits were obtained based on both plane-source and particulate-source models. Doses computed by the latter model are strongly dependent on fallout-particle-size distribution.

6. The models developed in the course of this study can be profitably applied to answer important questions pertaining to gamma/beta dose relationships, human vulnerability and cattle/sheep casualty assessments in the post-attack era.

ABSTRACT

Absorbed beta-radiation dose expected from fallout particles deposited on the skin was estimated by use of the Beta Transmission, Degradation and Dissipation (TDD) model and a Condensed-State Diffusion-Controlled model that describes the mechanism of fission-product absorption in fallout. A fission density of 10^{15} fissions per cubic centimeter of fallout material was assumed. Comparison of computed doses with the most recent experimental data relative to skin response to beta-energy deposition leads to the conclusion that even for fallout arrival times as early as 10^3 seconds (16.7 minutes post-detonation), no skin ulceration is expected from single particles 500 micron or less in diameter.

Doses were estimated for a limited number of particulate sources containing fractionated fission-product mixtures. Results indicate that extreme fractionation would cut down the beta dose by a factor of two.

Absorbed gamma doses calculated for one particle size (100μ) show a beta-to-gamma ratio of about 15. Dose ratio for larger particle sizes will be smaller.

Doses from arrays of fallout particles of different size distributions were computed, also, for several fallout mass deposition densities; time intervals required to accumulate doses sufficient to initiate skin lesions were calculated.

These times depend strongly on the assumed fallout-particle-size distribution. Deposition densities in excess of 100 mg per square foot of the skin will cause beta burns if fallout arrival time is less than about three hours, unless the particles are relatively coarse (mean particle diameter more than 250μ).

TABLE OF CONTENTS

ABSTRACT	i
LIST OF TABLES	iv
LIST OF FIGURES	v
I. INTRODUCTION	1
II. THE SINGLE-PARTICLE BETA-DOSE MODEL	2
III. EVALUATION OF THE SINGLE-PARTICLE MODEL	12
IV. EFFECT OF RADIONUCLIDE FRACTIONATION ON BETA DOSES FROM SINGLE PARTICLES	18
V. THE SINGLE-PARTICLE GAMMA-DOSE MODEL	21
VI. DOSE CRITERIA FOR SINGLE-PARTICLE EXPOSURE	24
VII. THE MULTIPLE-PARTICLE BETA-DOSE MODEL	25
VIII. DOSE CRITERIA FOR MULTIPLE-PARTICLE DEPOSITION	36
IX. RESULTS AND DISCUSSION	37
A. Beta Doses from Single Particles	37
1. Particles Containing Unfractionated Fission-Product Mixtures	37
2. Particles Containing Fractionated Fission-Product Mixtures	47

TABLE OF CONTENTS
(Continued)

B. Gamma Doses from Single Particles	49
C. Beta Doses From Multiparticle Fallout . .	53
X. CONCLUSIONS AND RECOMMENDATIONS	84
XI. REFERENCES.	89

LIST OF TABLES

1.	Nuclides Remaining at Particle Surface.	6
2.	Nuclides Uniformly Distributed Within Particle	7
3.	Nuclides With Both Surface and Interior Components Within the Particle.	8
4.	Particle Diameters and Grid Dimensions For Fallout Deposition Density of 1000 ng/ft ²	30
5.	Expected Retention Times of Particles on Human Skin	46
6.	Fraction of Atoms (F_p) That Exist in the Form of Refractory Elements at the Time of Solidification	48
7.	Beta Doses (Rads) From Fallout Particles Containing Unfractionated and Fractionated Fission-Product Mixtures	50
8.	Ratio of Beta Doses from Particles Containing Fractionated Fission-Product Mixtures to Beta Doses from Particles Containing Unfractionated Mixtures	51
9.	Gamma Doses from Fallout Particles.	52
10.	Effect of Exposure-Initiation Time on Krebs Doses Delivered to the Skin	81

LIST OF FIGURES

1.	Ratio of Calculated (TDD Model) Dose to Dose Measured with a β -Extrapolation Chamber (Tissue Depth of 30μ)	14
2.	Comparison of TDD Model Calculations with Monte-Carlo Calculations and Extrapolation-Chamber Measurements (Delay Time 5.75 hr)	15
3.	Comparison of Calculated (TDD Model) Dose Rates with Film Data (160μ Particles)	16
4.	Ratio of Model (TDD) Dose to Extrapolation-Chamber Dose, as a Function of Tissue Depth (236μ Particles)	17
5.	Schematic of the Multiple-Particle Array Concept	27
6.	Comparison between Doses Computed for a Plane Source and the Corresponding Values for a Multiparticle Source (Delay Time 10^3 Seconds, Deposition Density 100 mg/ft^2)	35
7.	Krebs Dose Delivered to the Skin by Single Fallout Particles (Exposure Starting Time: 10^3 Seconds After Detonation)	38
8.	Point Depth Dose Delivered to the Skin by Single Fallout Particles (Exposure Starting Time: 10^3 Seconds After Detonation)	39
9.	Krebs Dose Delivered to the Skin by Single Fallout Particles (Exposure Starting Time: 10^4 Seconds After Detonation)	40
10.	Point Depth Dose Delivered to the Skin by Single Fallout Particles (Exposure Starting Time: 10^4 Seconds After Detonation)	41
11.	Krebs Dose Delivered to the Skin by Single Fallout Particles (Exposure Starting Time: 10^5 Seconds After Detonation)	42

12.	Point Depth Dose Delivered to the Skin by Single Fallout Particles (Exposure Starting Time: 10^5 Seconds After Detonation).	43
13.	Krebs Dose Delivered to the Skin by Single Fallout Particles (Exposure Starting Time: 10^6 Seconds After Detonation).	44
14.	Point Depth Dose Delivered to the Skin by Single Fall- out Particles (Exposure Starting Time: 10^6 Seconds After Detonation).	45
15.	Point Depth Beta and Gamma Dose from a 100μ Particle	54
16.	Beta Dose Delivered to the Skin by Multiparticle Fall- out of 100μ Mean Diameter and 1000μ Maximum Diameter (Exposure Starting Time: 10^3 Seconds After Detonation)	55
17.	Beta Dose Delivered to the Skin by Multiparticle Fall- out of 250μ Mean Diameter and 1000μ Maximum Diameter (Exposure Starting Time: 10^3 Seconds After Detonation)	56
18.	Beta Dose Delivered to the Skin by Multiparticle Fall- out of 500μ Mean Diameter and 1000μ Maximum Diameter (Exposure Starting Time: 10^3 Seconds After Detonation)	57
19.	Beta Dose Delivered to the Skin by Multiparticle Fall- out of 700μ Mean Diameter and 1000μ Maximum Diameter (Exposure Starting Time: 10^3 Seconds After Detonation)	58
20.	Beta Dose Delivered to the Skin by Multiparticle Fall- out of 1000μ Mean Diameter and 2000μ Maximum Diameter (Exposure Starting Time: 10^3 Seconds After Detonation)	59
21.	Beta Dose Delivered to the Skin by Multiparticle Fall- out of 100μ Mean Diameter and 1000μ Maximum Diameter (Exposure Starting Time: 10^4 Seconds After Detonation)	60
22.	Beta Dose Delivered to the Skin by Multiparticle Fall- out of 250μ Mean Diameter and 1000μ Maximum Diameter (Exposure Starting Time: 10^4 Seconds After Detonation)	61
23.	Beta Dose Delivered to the Skin by Multiparticle Fall- out of 500μ Mean Diameter and 1000μ Maximum Diameter (Exposure Starting Time: 10^4 Seconds After Detonation)	62

24.	Beta Dose Delivered to the Skin by Multiparticle Fall-out of 700 μ Mean Diameter and 1000 μ Maximum Diameter (Exposure Starting Time: 10 ⁴ Seconds After Detonation)	63
25.	Beta Dose Delivered to the Skin by Multiparticle Fall-out of 1000 μ Mean Diameter and 2000 μ Maximum Diameter (Exposure Starting Time: 10 ⁴ Seconds After Detonation)	64
26.	Beta Dose Delivered to the Skin by Multiparticle Fall-out of 100 μ Mean Diameter and 1000 μ Maximum Diameter (Exposure Starting Time: 10 ⁵ Seconds After Detonation)	65
27.	Beta Dose Delivered to the Skin by Multiparticle Fall-out of 250 μ Mean Diameter and 1000 μ Maximum Diameter (Exposure Starting Time: 10 ⁵ Seconds After Detonation)	66
28.	Beta Dose Delivered to the Skin by Multiparticle Fall-out of 500 μ Mean Diameter and 1000 μ Maximum Diameter (Exposure Starting Time: 10 ⁵ Seconds After Detonation)	67
29.	Beta Dose Delivered to the Skin by Multiparticle Fall-out of 700 μ Mean Diameter and 1000 μ Maximum Diameter (Exposure Starting Time: 10 ⁵ Seconds After Detonation)	68
30.	Beta Dose Delivered to the Skin by Multiparticle Fall-out of 1000 μ Mean Diameter and 2000 μ Maximum Diameter (Exposure Starting Time: 10 ⁵ Seconds After Detonation)	69
31.	Beta Dose Delivered to the Skin by Multiparticle Fall-out of 100 μ Mean Diameter and 1000 μ Maximum Diameter (Exposure Starting Time: 10 ⁶ Seconds After Detonation)	70
32.	Beta Dose Delivered to the Skin by Multiparticle Fall-out of 250 μ Mean Diameter and 1000 μ Maximum Diameter (Exposure Starting Time: 10 ⁶ Seconds After Detonation)	71
33.	Beta Dose Delivered to the Skin by Multiparticle Fall-out of 500 μ Mean Diameter and 1000 μ Maximum Diameter (Exposure Starting Time: 10 ⁶ Seconds After Detonation)	72
34.	Beta Dose Delivered to the Skin by Multiparticle Fall-out of 700 μ Mean Diameter and 1000 μ Maximum Diameter (Exposure Starting Time: 10 ⁶ Seconds After Detonation)	73

35. Beta Dose Delivered to the Skin by Multiparticle Fall-out of 1000 μ Mean Diameter and 2000 μ Maximum Diameter (Exposure Starting Time: 10⁶ Seconds After Detonation) 74
36. Beta Dose Delivered to the Skin by Multiparticle Fall-out of 100 μ Mean Diameter and 1000 μ Maximum Diameter (Exposure Starting Time: 10⁷ Seconds After Detonation) 75
37. Beta Dose Delivered to the Skin by Multiparticle Fall-out of 250 μ Mean Diameter and 1000 μ Maximum Diameter (Exposure Starting Time: 10⁷ Seconds After Detonation) 76
38. Beta Dose Delivered to the Skin by Multiparticle Fall-out of 500 μ Mean Diameter and 1000 μ Maximum Diameter (Exposure Starting Time: 10⁷ Seconds After Detonation) 77
39. Beta Dose Delivered to the Skin by Multiparticle Fall-out of 700 μ Mean Diameter and 1000 μ Maximum Diameter (Exposure Starting Time: 10⁷ Seconds After Detonation) 78
40. Beta Dose Delivered to the Skin by Multiparticle Fall-out of 1000 μ Mean Diameter and 2000 μ Maximum Diameter (Exposure Starting Time: 10⁷ Seconds After Detonation) 79

I. INTRODUCTION

In 1954, residents of Rongelap Atoll in the Marshall Islands were exposed to fallout which arrived within hours after detonation of the CASTLE BRAVO nuclear device. Several of the Atoll's inhabitants suffered severe skin burns. Primarily as a result of this experience, the possibility of "beta burn" from nuclear fallout has been recognized. However, to date attempts to predict the acute or chronic skin effects that might be expected following exposure to fallout have been limited. This limitation results mainly from the lack of experimental data on the biologic response of the skin to particulate-source exposures, from incomplete understanding of the relationship of such response to that encountered in other localized exposures (e.g. collimated x-ray beams) for which data are available, and from the absence of reliable beta-dose calculational models. All of these are required in order to relate dose to observed effect in a manner that allows prediction of the biological effects from knowledge of the expected fallout interaction.

The literature indicates that work on the theoretical aspects of the beta-dose problem has progressed faster than have experimental efforts. As early as 1956 Loevinger, Japha and Brownell devised an analytical representation (model) to calculate beta doses from "discrete radioisotope sources".⁽¹⁾ By 1966, four models were available.⁽²⁾ Of these models, the most precise, though complex, is the Transmission, Degradation, and Dissipation (TDD)⁽²⁾ model. The present paper, based on the TDD model, presents predicted beta doses which would result from skin deposition of nuclear-weapon fallout particles.

It is expected that a nuclear attack on the United States would result in low-intensity gamma-radiation fields over much

of the fallout area which would develop. Exposure to the low-intensity field would pose little or no immediate or long-term whole-body gamma-radiation hazard. However, it has been suggested that in such situations contact of individual fallout particles with exposed skin could constitute a potential hazard. Individual particles may deposit on the skin via direct deposition during passage of the fallout cloud, or following resuspension of particles at a later time.

Each particle, if radioactive enough, is capable of producing a lesion. Several particles could reside in the same general skin area; if they are close enough, their effects could be additive, in the sense of causing one lesion. However, at larger particle-separation distances, beta-radiation dose deliveries would not interact. That is, the dose contribution from one particle to the tissue in the vicinity of another particle would be negligible. This situation will be treated separately in Sections II through VI. At small particle-separation distances, estimation of the dose delivered at any point in tissue would require summation of the dose contributions from all particles in the immediate vicinity. This latter situation is treated separately in Sections VII and VIII.

II. THE SINGLE-PARTICLE BETA-DOSE MODEL

The TDD model (for single particles) is composed of six separate semi-independent computer codes. The first (Code 1) is a nuclide-abundance code which calculates the activity of each radionuclide generated in the detonation of a nuclear device or weapon. This code also considers radioactive decay and calculates fission-nuclide activity at any post-detonation time.

Code 2 computes the beta spectrum for each beta-emitting nuclide, given the end-point energies, beta branching fractions and degree of forbiddenness of the beta transitions⁽³⁾. Output from this code is a sequence of values representing the probability that a beta particle will be emitted with an energy between E and $E + \Delta E$, where $\Delta E = 0.04$ Mev, and where values for E range from 0 to the maximum β -energy, E_{\max} . Individual fission-product beta spectra have been generated and are stored on tape for use with the composite spectrum code (Code 3).

Code 3 is a composite-spectrum routine which sums the individual beta spectra of the fission-product nuclides with appropriate weighting for the activity of each contributing nuclide, as determined by Code 1. Code 3 produces a point-source beta spectrum at a given time for the specific weapon under consideration. Output from this code is a sequence of values representing the number of betas, per energy interval, emitted by the source.

The electron spectrum from a fallout particle (assumed to be spherical in shape) differs from that produced by a point source because scattering and absorption processes within the particle degrade the spectrum. Calculation of the extent of degradation is complicated by the fact that in fallout particles some fission products are uniformly distributed within the particle material, others have condensed on the particle surface, while the rest behave in an intermediate fashion.⁽⁴⁾

Korts and Norman developed a model⁽⁵⁾ - termed the Condensed State Diffusion Controlled Model - that describes the mechanism of fission-product absorption in fallout material distributed in a radioactive cloud following a nuclear detonation. In this model they assumed that: a. the fallout material is glassy silicate; b. the surface of a fallout particle is in equilibrium

with the gas phase; and c. the rate of transfer of fission products into the interior of the fallout particle is diffusion controlled. One output of this Condensed State Diffusion Controlled Model consists of a set of radial fission-product-concentration profiles in fallout particles of different sizes. Based on such concentration profiles, Korts and Norman calculated for each fission product the percentage of total nuclide present that would diffuse into the particle. In almost all cases examined, it was found that "loadings" of 0, 25, 50, 62.5, 75, 82.5 and 100% (by weight) could be used to describe the portion of fission product present diffusing into the particle. (The complementary percentage, in each of the 7 classes, represents the portion of the fission product present that remains at the particle surface). Zero-percent diffusion takes place when the fission product condenses on the particle surface, essentially without any diffusion during particle cooling; while 100% diffusion represents complete diffusion, leading to homogeneous distribution of the fission product in the silicate matrix. This Condensed State Diffusion Controlled Model was used, in the manner described below, to provide the geometric basis for the electron degradation within fallout particles.

Degradation suffered by the emanating electron spectrum is handled by Code 4, a Monte-Carlo program which starts with a given number of emitted betas in a specified energy interval and then computes the loss in electron energy and number due to scattering and absorption processes within the particle. The code outputs two sets of Monte-Carlo-determined energy-dependent loss coefficients; set A for the homogeneously-distributed fission-product case, and set B for the surface-condensed case. These coefficients are then applied to the composite beta spectrum from the point source of fission products (Code 3) by Code 5. Application of these loss factors is straightforward

for the 0% and 100% diffusion cases (in which set B and set A, respectively, are utilized). For five intermediate diffusion cases, set A was applied to the percentage diffusing into the particle, while set B was applied to the percentage remaining at the surface. Output of Code 5 thus consists of a degraded beta spectrum emerging from a fallout particle of a specified size.

Tables 1, 2 and 3 list, respectively, (1) nuclides which remain entirely at the particle surface, (2) nuclides which distribute uniformly within the particle, and (3) nuclides with both surface and interior components within the particle*.

*Latest modifications in the Condensed State Diffusion Controlled model may cause a few changes in the "loadings" of some nuclides. However, such changes will not affect the dose calculations to any appreciable extent.

TABLE 1

Nuclides Remaining at Particle Surface*

Se - 83
Er - 83,84,85,87
Kr - 85,87,88,89
Rb - 87,88,89
Sr - 89
Ru - 107,108
Rh - 108
Pd - 107
I - 135
Xe - 135,137,138
Cs - 135,136,137,138,139
Ba - 139

*Energy states of the nucleus do not affect the behavior of the nuclide from the viewpoint of diffusion within the particle core.

TABLE 2

Nuclides Uniformly Distributed Within Particle

Zn - 72
Ga - 72,73,74,75,76
Ge - 75
Y - 94,96
Zr - 95,97
Nb - 95,97,99,100
Mo - 99,101,102
Tc - 99,101,102
Sb - 126
La - 143
Ce - 143,144,145,146
Pr - 143,144,145,146
Nd - 147,149,151
Pm - 147,149,150,151,152,153,154
Sm - 151,153,155,156
Eu - 155,156,157,158,159,160
Gd - 159,161
Tb - 160,161

TABLE 3

Nuclides With Both Surface and Interior
Components Within the Particle

<u>Nuclide</u>	<u>Fraction on Surface</u>
Ge-77	0.250
As-77	0.250
Ge-78	0.250
As-78	0.250
As-79	0.500
Se-79	0.500
As-81	0.500
Se-81	0.500
Sr-90	0.750
Y-90	0.750
Kr-91	0.500
Rb-91	0.500
Sr-91	0.500
Y-91	0.500
Sr-92	0.500
Y-92	0.500
Y-93	0.250
Zr-93	0.250
Tc-103	0.250
Ru-103	0.250
Tc-104	0.250
Ru-105	0.250
Rh-105	0.250

TABLE 3 (Cont'd)

<u>Nuclide</u>	<u>Fraction on Surface</u>
Ru-106	0.750
Rh-106	0.750
Pd-109	0.875
Pd-111	0.750
Ag-111	0.750
Pd-112	0.625
Ag-112	0.625
Pd-113	0.625
Ag-113	0.625
Pd-114	0.625
Ag-114	0.625
Ag-115	0.500
Cd-115	0.500
In-115	0.500
Ag-116	0.625
Cd-117	0.625
In-117	0.625
Cd-118	0.625
In-118	0.625
In-119	0.625
In-120	0.500
In-121	0.500
Sn-121	0.500
In-123	0.250

TABLE 3 (Cont'd)

<u>Nuclide</u>	<u>Fraction on Surface</u>
Sn-123	0.250
Sb-124	0.250
Sn-125	0.250
Sb-127	0.250
Te-127	0.250
Sb-128	0.250
Sb-129	0.500
Te-129	0.500
I-129	0.500
I-130	0.500
Te-131	0.500
I-131	0.500
Te-132	0.500
I-132	0.500
Te-133	0.500
I-133	0.500
Xe-133	0.500
I-134	0.750
Ba-140	0.750
La-140	0.750
Ba-141	0.500
La-141	0.500
Ce-141	0.500
La-142	0.250

Code 6 operates on the resulting composite degraded spectrum to compute the depth dose rate in tissue. This is based on energy-dissipation factors for fast electrons as calculated by L. V. Spencer in NBS Monograph 1⁽⁶⁾.

The dose-rate, D_t (in rads per hour), at a tissue depth Z cm from a particle of volume V cm³, emitting $N_e(E_0)$ beta particles/sec-cm³ in the energy interval ΔE with mean energy E_0 , in Mev (this is the emerging degraded spectrum in the present work), is given by:

$$D_t = \frac{kfgV}{4\pi Y^2} \sum_{E_0=\Delta E/2}^{E_0=E_{\max}-\Delta E/2} J(x) (dE/dr)_{E_0} N_e(E_0) \quad (1)$$

where k is a constant, which has a value of 5.76×10^{-5} rad·g·sec/Mev-hr, relating energy-transport rate to dose rate.

f designates a dimensionless correction factor for a semi-infinite absorber, determined from an auxiliary Monte-Carlo program.

g is the ratio of dose rate at a distance Y (cm) from the center of a spherical source (radius R (cm)) to the dose rate from a point source at the same distance ($Y > R$); the ratio is a dimensionless quantity given by the equation:

$$g = \frac{3Y^2}{R^2} \left[0.5 + \left(\frac{R^2 - Y^2}{4RY} \right) \ln \left(\frac{Y + R}{Y - R} \right) \right] \quad (2)$$

$J(x)$ represents Spencer's energy-dissipation-distribution function evaluated at tissue depth Z measured in units of the normalizing residual range, r_0 ; $x = Z\rho/r_0$, ρ being the density of the absorbing medium⁽⁶⁾.

$(dE/dr)_{E_0}$ is the stopping power of the absorber for electrons emitted from the particle with energy E_0 .

The resulting dose rates, summed over the composite degraded spectrum, form the output of this part of the model.

The final operation of the composite TDD model integrates the various dose rates (from each energy interval) computed via Equation 1 over time to get the total absorbed dose. In practice, in order to reduce computation time, the integration is carried out by the use of time-integrated beta activities derived from the inventory code (Code 1) to make up a time-integrated composite beta spectrum, which is then degraded and deposited in tissue as explained above. That is, the time-integration is done from the start rather than at the last step.

Recently, the six codes have been unified into a single modified composite program to reduce computer run-time⁽⁷⁾. Also, several new features have been introduced into the composite program to increase its ability to cope with a variety of beta dose problems⁽⁸⁾.

III. EVALUATION OF THE SINGLE-PARTICLE MODEL

Validity of the TDD-model dose predictions has been examined⁽⁸⁾ through comparison of the model-computed doses delivered by reactor-irradiated uranium carbide particles with:

a. Doses from the UC_2 particles measured with a β -extrapolation chamber⁽⁹⁾; b. UC_2 -particle dose values obtained by a photographic-film dosimetry technique; and c. Dose values computed through application of a completely independent Monte-Carlo calculational technique.

Tests included doses at shallow as well as at relatively large depths (7500μ) in tissue, at points directly underneath the particle and points radially displaced to distances as far as 5000 microns. Particles of variable sizes, and reactor irradiation times of different duration, were also included in the comparisons.

Typical results obtained in the comparisons with data from the extrapolation chamber, the Monte-Carlo program, and the photographic-film exposure technique are presented in Figures 1, 2 and 3, respectively. The primary conclusions drawn from the comparisons were⁽⁸⁾:

1. On the whole, agreement between values obtained through use of the composite program and by experimentation (and exercise of the cited Monte Carlo program) was satisfactory.

2. The ranges of particle sizes (85μ to 310μ) and time periods of reactor irradiation (5 min to 24 hr) considered appear to have little influence on the extent of agreement achieved.

3. Tissue beta-radiation delivery, i.e., absorption, estimated by the composite TDD model for shallow tissue depths is invariably higher than that derived from the Monte Carlo calculations. As the tissue depth considered increases, agreement between the TDD model and experimental results improves until (as shown in Figure 4), at a tissue path length of about

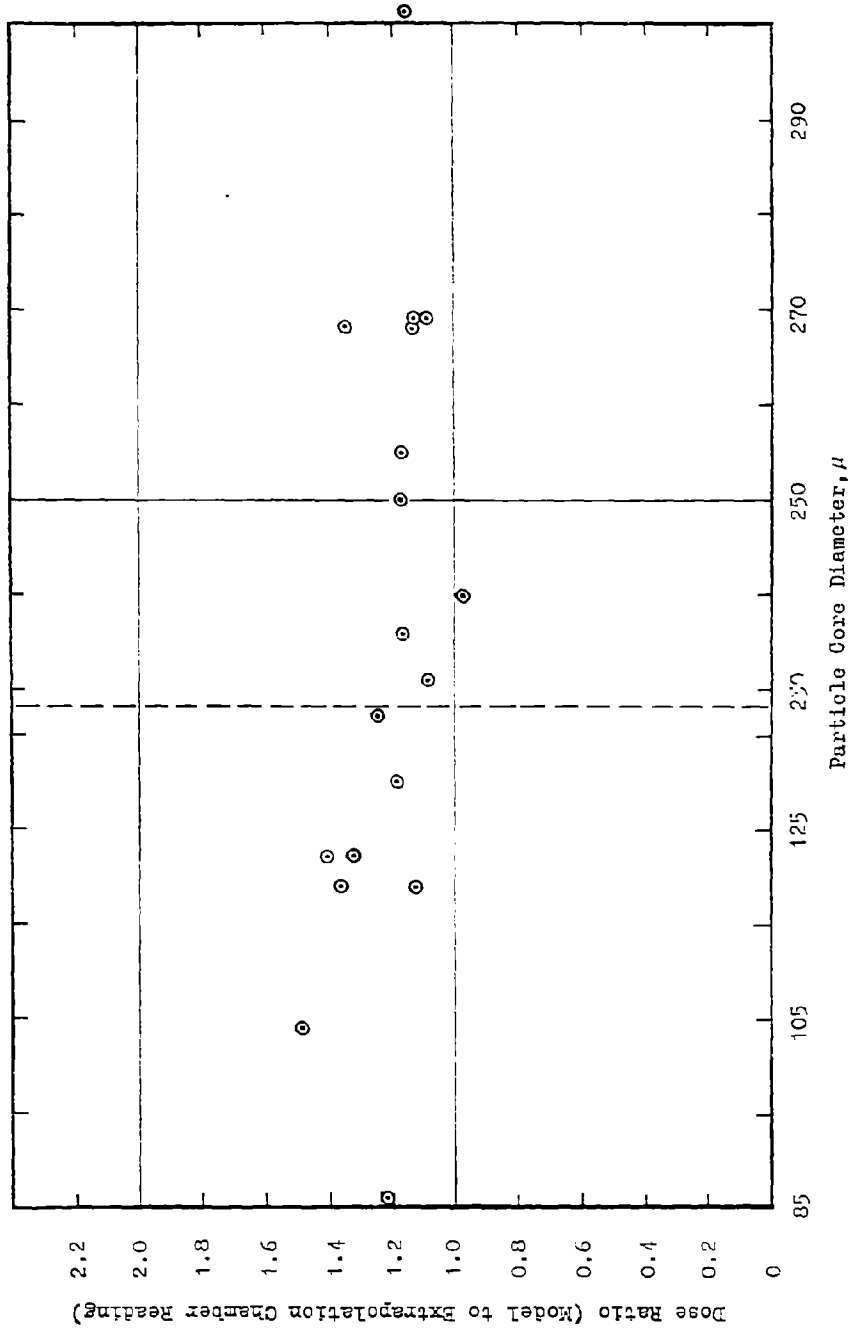


Figure 1
 Ratio of Calculated (TDD Model) Dose to Dose
 Measured with a β -Extrapolation Chamber
 (Tissue Depth of 30 μ)

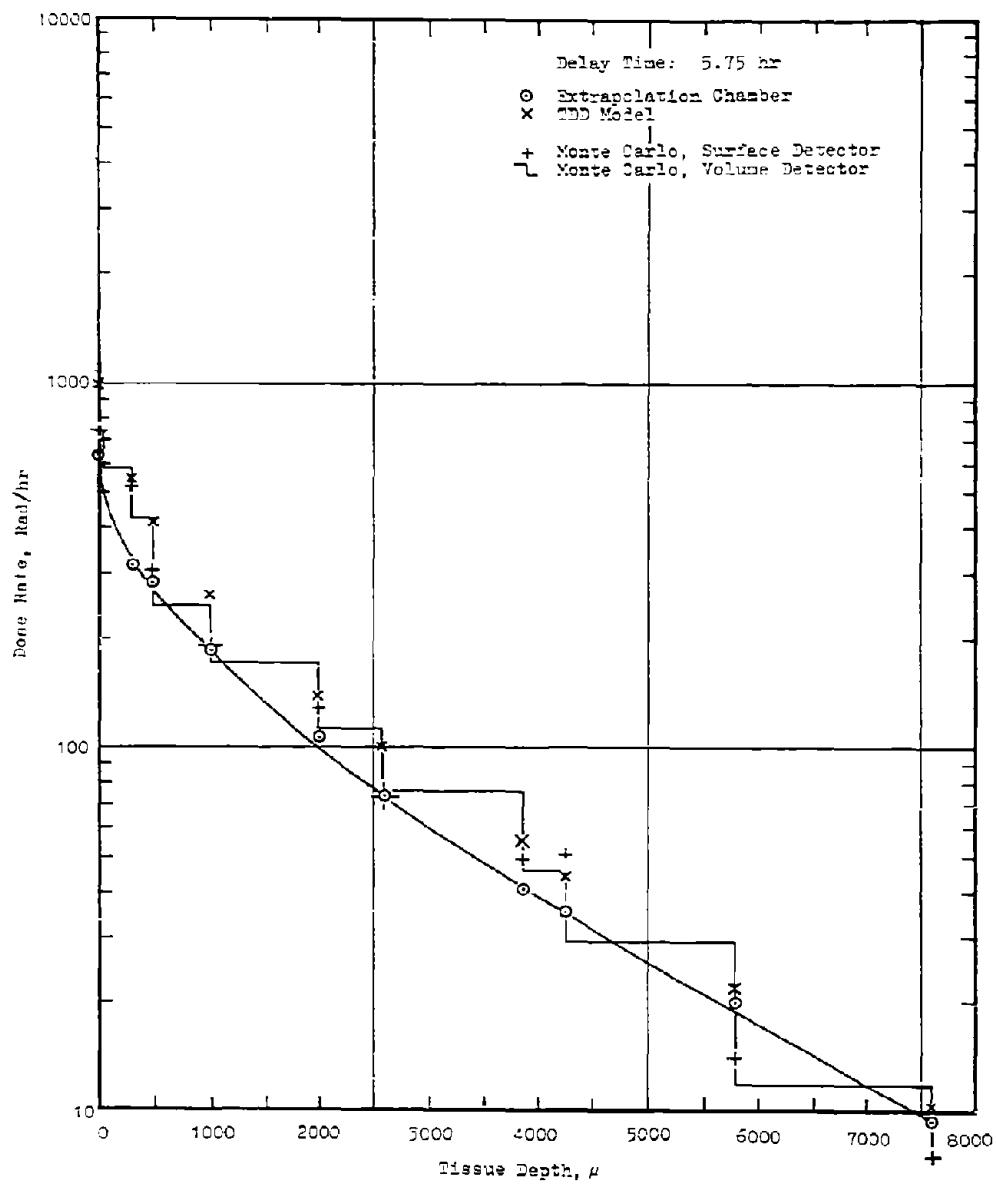


Figure 2
 Comparison of TDD Model Calculations
 with Monte-Carlo Calculations and
 Extrapolation-Chamber Measurements

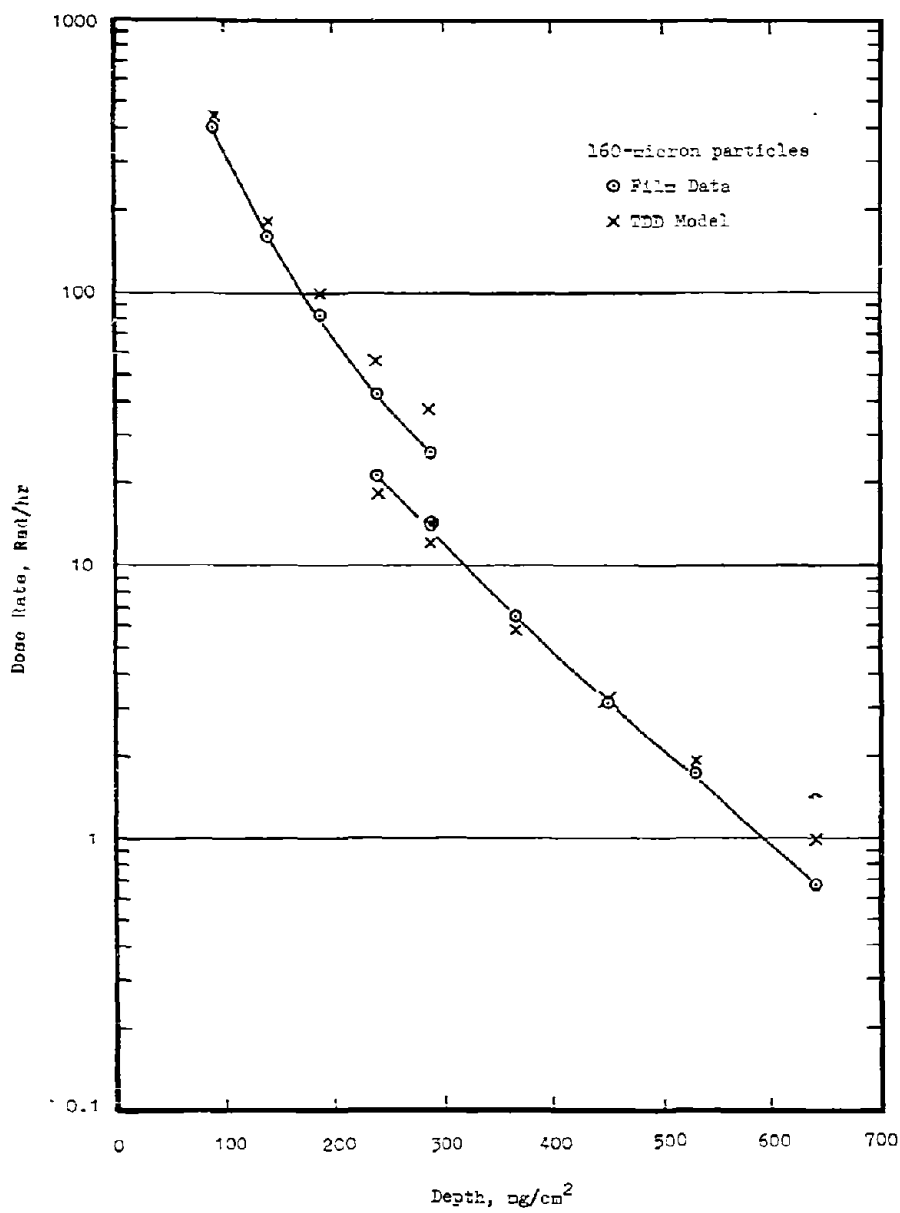


Figure 3
 Comparison of Calculated (TDD Model)
 Dose Rates with Film Data

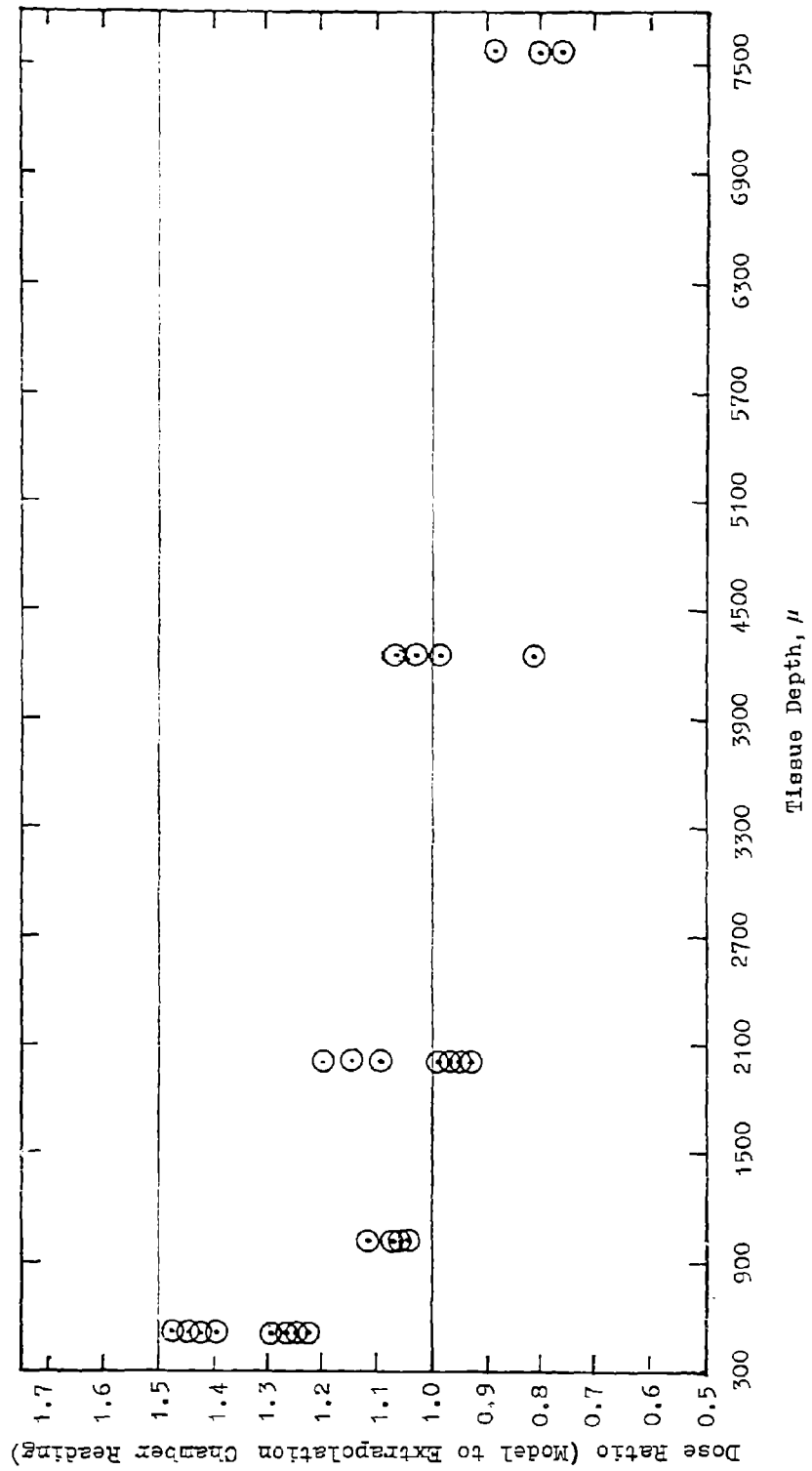


Figure 4
 Ratio of Model (TDP) Dose to Extrapolation-Chamber Dose, as a Function of Tissue Depth
 ($^{236}\mu$ Particles)

4000 microns, the model and test-method values tend to agree. Such relationships are interpreted as indications that the model underestimates electron attenuation in the particle material and overestimates that in tissue.

4. Delay times (time periods between termination of reactor irradiation and start of tissue exposure) greater than approximately 25 hours appear to increase the difference between model predictions and values determined by the test methods, but not to an appreciable degree.

5. Doses measured directly below the particle by photographic-film experiments agree rather well with model predictions. An exception to this is for dose locations very close to the particle, in which situation apparent saturation of film occurs.

IV. EFFECT OF RADIONUCLIDE FRACTIONATION ON BETA DOSES FROM SINGLE PARTICLES

For a land-surface nuclear detonation, local fallout consists of the larger radioactive particles formed in the explosion. Because of radionuclide fractionation, local fallout is depleted in volatile nuclide mass-chains (such as mass-89 chain) relative to refractory mass chains (such as mass-95 chain). Worldwide fallout, on the other hand, consists of the smaller particles of debris; it is relatively enriched in volatile mass chains. The effect of fractionation on beta doses from fallout particles is to produce a variation in the dose delivered by particles of the same size containing the same number of equivalent fissions (based on abundance of refractory mass chains). The difference between doses from unfractionated and fractionated particles depends on the extent of fractionation.

For estimation of beta doses from fallout particles containing fractionated fission-product mixtures, a suitable method had to be found for estimating the radiochemical composition of these fractionated mixtures; then the doses had to be calculated by the same method described in Section II above.

Freiling, et al.⁽¹⁰⁾ suggested a semiempirical approach to estimate the radionuclide abundance in fission-product mixtures fractionated to variable degrees. Their approach can be summarized as follows:

1. Consider only those nuclides which, at some time in the fallout-particle history, contribute significantly to the dose rate. These nuclides and their isobars form the significant mass chains.

Although some 90 mass chains are produced in the thermal-neutron fission of ^{235}U , only about half of these make, at some time or another, a significant contribution to the dose rate. Calculations can be considerably shortened* by consideration of these mass chains only.

2. Divide the fission-product elements into refractory and volatile groups according to their vapor pressures at the solidification temperature of the soil pulled upward into the cloud.

The chosen temperature used in the calculations reported is 1400°C , the solidification point of an idealized silicate soil⁽⁴⁾. Volatile elements are those whose predominant species have a normal boiling point below 1400°C . These elements are: As, Se, Br, Kr, Rb, Mo, Tc, Te, I, Xe and Cs. All other elements are considered refractory.

* This approximation was used for estimation of beta doses from fractionated particles only.

In any mass chain, the fraction, F_R , of atoms that exist in the form of refractory elements at the time of solidification (time at which 1400 °C is reached by the cooling fireball), t , is a measure of the refractory nature of that mass chain taken as a whole. The value of t is given by the equation⁽⁴⁾:

$$t \text{ (sec)} = 1.88 W^{0.363}$$

where W is the total yield of the weapon in kiloton (Kt). For 25 Kt and 5 Mt weapons, this equation gives solidification times of 6 and 41 seconds, respectively.

Values of F_R were calculated for the significant mass chains by Freiling⁽¹⁰⁾, on the basis of the tables devised by Bolles and Ballou⁽¹¹⁾. From these tables, Freiling obtained the number of atoms of each fission-product mass chain present in various elemental forms at 6 and 41 seconds following ^{235}U -thermal-neutron fission. The elemental distributions had been calculated by Bolles and Ballou according to both Present's minimum-kinetic-energy theory of charge distribution⁽¹²⁾ and the equal-charge-displacement theory of Glendenin, Coryell and Edwards⁽¹³⁾. Freiling carried out calculations of F_R on both bases. However, since Glendenin's theory is generally preferred, the calculations made in this report are based on that treatment only.

3. Define the abundance of each nuclide in the fractionated mixture as the product of its abundance in the corresponding unfractionated mixture (at the solidification time) and a Fractionation Correction Factor, $(r_{89,95})^1 - b_k$, where:

$r_{89,95}$ is the fractionation ratio, or the ratio of the number of fissions required to produce the quantity of mass-89 chain found in a particular fission-product mixture (sample, particle) to the number required to produce the quantity of mass-95 chain in the same mixture, and

b_k is an empirical correlation parameter observed to be approximately equal to $\sqrt{F_R}$ * in debris from high-yield surface bursts⁽¹⁴⁾.

Figure 5 of reference 10 relates these Fractionation Correction Factors to the fractionation ratio $r_{89,95}$ for different values of F_R . With the fractionation ratio parameterized, the correction factors used in the dose calculations reported here were obtained from that Figure and inputted into the Single-Particle TDD model, which then calculated the fractionated nuclide inventory at t , calculated the beta spectrum of the mixture at that point in time, decayed it to the desired delay time, integrated it over the desired exposure time and finally proceeded to calculate the beta dose from the particle in the manner described previously in Section II. Nuclide diffusion into the fallout particle was taken into account and was handled as explained in Section II.

V. THE SINGLE-PARTICLE GAMMA-DOSE MODEL

One of the questions frequently asked about exposure of human skin to radiation from fallout particles is: What is the relative contribution of γ -radiation to the total absorbed dose in skin? Is it sufficiently significant so that it should always be calculated and added to the beta dose before the biological consequences of exposure can be evaluated?

* This relation is approximate. It neglects, among other things, the change of b_k with fallout-particle size. It is, however, adequate for the present calculations.

For answers to these questions, a calculational program had to be written to estimate the gamma-radiation dose from a point source containing a mixture of ^{235}U -thermal-neutron-fission products. Similar to the beta program, this program is a combination of several codes, as follows:

Code 1 is a fission-product abundance code identical to Code 1 of the beta-dose model. It creates and maintains a library of fission yields, accepts a library of nuclear constants, produces a set of possible decay modes for the nuclides in the library, calculates nuclide inventories immediately after fission and applies the generated decay schemes to the fission yields to calculate inventories of nuclides at requested delay times.

Code 2 is an individual-nuclide-gamma-spectrum code which stores the gamma spectrum of each nuclide in terms of the number of photons in each energy interval.

The information from Codes 1 and 2 is combined into a composite γ -spectrum code (Code 3). This yields a time-integrated gamma-spectrum which is a properly weighted composite of all the individual gamma spectra from the fission-product mixture of nuclides in the point source of interest.

The last code (Code 4) calculates the gamma dose at specified depths in tissue, with the equation:

$$\begin{aligned}
 D_{\gamma} \text{ (rad)} &= \left[\frac{S}{4\pi r^2} (e^{-\Sigma_t r}) B_r (\Sigma_t r, \bar{E}_{\gamma}) \bar{E}_{\gamma} \right] \frac{\Sigma_a C^*}{\rho} \\
 &= \left[\frac{S \bar{E}_{\gamma} \Sigma_a C^*}{4\pi \rho} \right] \left\{ \frac{e^{-\Sigma_t r} B_r (\Sigma_t r, \bar{E}_{\gamma})}{r^2} \right\} \quad (3)
 \end{aligned}$$

- where:
- S is the total number of gammas produced in the energy interval "centered" on \bar{E}_γ , during the exposure period
 - R is the distance from source to target or dose point p, cm
 - Σ_t is the total macroscopic cross section for all processes of attenuation (including scattering, Σ_s), cm^{-1}
 - Σ_a is equal to $(\Sigma_t - \Sigma_s)$, the macroscopic cross section for gamma absorption in the medium surrounding p, cm^{-1}
 - ρ is the density of medium through which the gammas pass and in which they are absorbed, g/cm^3
 - \bar{E}_γ is the average gamma energy of the energy interval considered, Mev
 - $B_r(\Sigma_t r, \bar{E}_\gamma)$ is the dose buildup factor, dimensionless
 - G^* is the conversion factor from Mev/gram to rad; it is equal to 1.602×10^{-8}

Values of S were provided by the previously described codes for energy intervals of 0.1 Mev. The macroscopic cross sections $\Sigma_t^{(15)}$ and $\Sigma_a^{(16)}$ for water were used in the absence of more precise values for tissue. Similarly, the density, ρ , was taken as 1 gram/cm^3 , and the buildup factors were those of water, obtained from reference 15.

VI. DOSE CRITERIA FOR SINGLE-PARTICLE EXPOSURE

Serious acute lesions of the skin are induced primarily by the destruction of the germinal cells of the epithelium. In humans, the subsurface depth of the skin germinal-cell layer varies between 20 and 250 microns. However, for convenience, a single depth of 100μ is usually chosen to represent the critical level. The absorbed beta dose (or amount of beta energy absorbed in an infinitesimally small mass of tissue surrounding the point of interest) at the point 100μ deep "underneath" the source (fallout particle) is termed the "Point Depth Dose" at 100μ .

For a considerable period of time, beta-radiation damage to skin was viewed almost entirely in terms of the estimated 100μ point depth dose. However, within recent years, it has become generally accepted that, for a serious radiation lesion to occur, the germinal cells must be destroyed over an area of skin too large for normal regeneration to replace them within a reasonable period of time. Of necessity, this has led to consideration of area dose absorption (specified by dose at the periphery) rather than dose absorbed at a specific point.

A survey by Krebs⁽¹⁷⁾ in 1967 showed that for an acute lesion of the skin to develop, the viable germinal cells must be reduced to a survival level of less than 0.001 over an area sufficiently large to prevent replacement of dead cells (via cell proliferation) in the margin of the exposure field. The criterion recommended by Krebs is that a 1500 rad or greater dose to the skin, deposited at any point of the equi-dose circle on the periphery of a 4 mm radius circular field 100μ deep in tissue, constitutes a potential skin-damage threat.

Krebs derived his conclusions from x-ray microbeam studies. At the time of his evaluation, little biological-damage data was available from single-particle investigations. Following publication of Krebs's conclusions, an experimental study to test the suggested criterion was conducted.⁽¹⁸⁾ Irradiated microspheres were used as radiation sources; swine were the experimental animals. Results obtained in this study showed that the minimum radiation dose, deposited at the periphery of a 4 mm radius field, required to produce a very small ulcer (less than 0.5 mm in diameter) is below 405 rads estimated. An ulcer one mm in diameter was produced following absorption of 660 rads (same field), a 2 mm diameter ulcer by about 1150 rads, etc. If one assumes linearity of the ulcer diameter with (4 mm radius field) dose (as indicated by the data), then by extrapolation a 350 rad delivery would just yield a zero-diameter ulcer.

In the work herein discussed, the 660 rad dose was used as the threshold dose for damage to human skin from deposited fallout particles. This admittedly arbitrary threshold was chosen on the basis that a one-millimeter diameter ulcer is small enough to be considered a threshold for damage but large enough to be recognizable. Choice of 350 or 1150 rads as a threshold dose does not appreciably affect the conclusions derived in Section IX below.

VII. THE MULTIPLE-PARTICLE BETA-DOSE MODEL

The multiple-particle beta-dose model is designed for evaluation of dose situations in which the fallout-particle deposition density on the skin is of such magnitude that beta radiation emitted from adjacent particles is absorbed in the same tissue volume.

Two distinct approaches can be used to examine the absorbed dose from multiparticle sources. In the first, the source is viewed as a uniform plane source of strength dependent only on the number of "equivalent fissions" of fission products deposited per unit area. In the more realistic second approach, the source is taken to be a group of fallout particles of size distribution dependent on the weapon yield and the distance from ground zero to the deposition point of interest. The beta dose delivered by such a source to the skin depends, in addition to the particle-size distribution, on the fallout mass deposited per unit area, and on the specific activity of the fallout.

The plane-source approach was pursued by Brown⁽¹⁹⁾, who used Spencer's plane-source calculations to compute beta-dose-rate multipliers for each fission-product beta emitter. Brown considered two situations: a. contact dose, where the plane source lies between an absorbing medium and a backscatterer; and b. beta bath, where an attenuation medium separates the absorbing medium from the plane source.

By use of Brown's contact-dose multipliers and the output from the abundance code (Code 1) of the TDD program, it was possible to calculate the dose delivered to the skin from a plane source of the desired activity level. Results of these computations are considered later in this Section.

In the second, or particulate, model, the source is viewed, for purpose of analytical examination, as consisting of superimposed strata of fallout particles, each stratum being in contact with the skin surface. Each stratum consists of an array of equal-size particles, with separate particles placed at the intersections of a uniform rectangular plane grid. Figure 5 illustrates the concept. The dose is estimated at point X, 100 μ below the central point of the grid plane. By summation of the dose contributions from individual particles as computed by the TDD model, the dose at X can be determined.

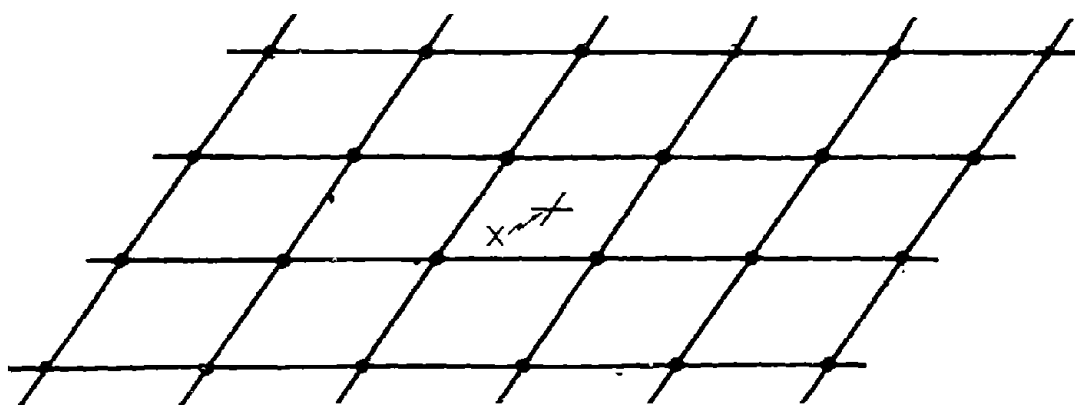


Figure 5
Schematic of the Multiple-
Particle Array Concept

For calculation of the dose at X, dose contributions from the particles closest to X are computed and added. Then doses from particles at increasing distances from X are added until the incremental increase in dose falls below a predetermined fraction of the initial sum, at which time the calculation stops.

For accuracy, 10 strata of arrays were considered in the calculations herein reported. Each stratum was assumed to contain 10% of the total fallout mass deposited (on a unit-area basis). Particle sizes for the arrays were determined as follows:

1. Assume a mean and a maximum particle size for the fallout deposit. In the first four situations considered, the means were taken parametrically as 100, 250, 500 and 700 μ , each with a fixed maximum of 1000 μ . In a fifth case the mean was 1000 and the maximum 2000 μ .

2. Assuming a log-normal distribution⁽⁴⁾ of particle sizes in each case, and with the knowledge of the maximum and the mean, trace a log-probability line for the particle-size distribution.

3. Subdivide the line into 10 equal-probability regions and determine the particle size, in each region, corresponding to the midrange probability. Use these 10 mean particle sizes for the strata.

Table 4 shows the particle size, and dimension of unit cell, for each of the ten particle-size classes of each of the five parametric-distribution cases. In all five cases shown the fallout deposition density was taken as 1000 mg/ft^2 . A similar set of values was obtained for each of the other five deposition densities (100, 200, 500, 2000 and 5000 mg/ft^2).

Two facts are worth mentioning here: 1. For obvious reasons the particulate approach is much more realistic than the plane-source approach; 2. For the same number of equivalent fissions per unit area, the plane-source computations give dose values higher than the Multiparticle Model by as much as an order of magnitude (see Figure 6). The discrepancies are due to both the geometry and the attenuation within particles. The detailed differences between the dose values resulting from the two approaches depend on the particle-size distribution assumed in the particulate approach (Figure 6). For a fixed maximum size, the difference decreases as the mean particle size decreases, but for the cases considered, a factor of 5 was the smallest encountered.

TABLE 4

Particle Diameters and Grid Dimensions
For Fallout Deposition Density of 1000 mg/ft²

Case 1: Mean Particle Diameter: 100 μ
Maximum Particle Diameter: 1000 μ

Class	Particle Diameter, μ	Grid Dimension, cm *
1	19.6	1.00×10^{-2}
2	35.9	2.37×10^{-2}
3	51.3	4.05×10^{-2}
4	68.3	6.24×10^{-2}
5	88.5	9.14×10^{-2}
6	113.2	1.32×10^{-1}
7	146.6	1.95×10^{-1}
8	194.9	2.99×10^{-1}
9	278.9	5.12×10^{-1}
10	509.4	1.27×10^0

* Grids are assumed to have square geometry. The dimension given is the length of the side of the square in cm.

TABLE 4
(Continued)

Case 2: Mean Particle Diameter: 250 μ
Maximum Particle Diameter: 1000 μ

Class	Particle Diameter, μ	Grid Dimension, cm
1	93.6	1.00×10^{-1}
2	134.7	1.72×10^{-1}
3	167.1	2.34×10^{-1}
4	198.7	3.09×10^{-1}
5	231.8	3.90×10^{-1}
6	269.4	4.88×10^{-1}
7	314.5	6.13×10^{-1}
8	373.6	7.95×10^{-1}
9	463.6	1.10×10^0
10	666.2	1.89×10^0

TABLE 4
(Continued)

Case 3: Mean Particle Diameter: 500 μ
Maximum Particle Diameter: 1000 μ

Class	Particle Diameter, μ	Grid Dimension, cm
1	306.2	5.88×10^{-1}
2	367.2	7.65×10^{-1}
3	409.0	9.11×10^{-1}
4	445.8	1.03×10^0
5	481.6	1.16×10^0
6	509.0	1.30×10^0
7	560.8	1.46×10^0
8	611.3	1.66×10^0
9	680.9	1.96×10^0
10	816.2	2.56×10^0

TABLE 4
(Continued)

Case 4: Mean Particle Diameter: 700 μ
Maximum Particle Diameter: 1000 μ

Class	Particle Diameter, μ	Grid Dimension, cm
1	543.9	1.40 x 10 ⁰
2	597.2	1.61 x 10 ⁰
3	631.2	1.75 x 10 ⁰
4	659.8	1.87 x 10 ⁰
5	686.6	1.98 x 10 ⁰
6	713.6	2.10 x 10 ⁰
7	742.6	2.23 x 10 ⁰
8	776.2	2.39 x 10 ⁰
9	820.6	2.60 x 10 ⁰
10	900.8	2.98 x 10 ⁰

TABLE 4
(Continued)

Case 5: Mean Particle Diameter: 1000 μ
Maximum Particle Diameter: 2000 μ

Class	Particle Diameter, μ	Grid Dimension, cm
1	612.6	1.67×10^0
2	754.3	2.20×10^0
3	817.9	2.58×10^0
4	891.5	2.93×10^0
5	963.2	3.29×10^0
6	1038.2	3.67×10^0
7	1121.6	4.15×10^0
8	1222.6	4.72×10^0
9	1361.8	5.53×10^0
10	1632.5	7.28×10^1

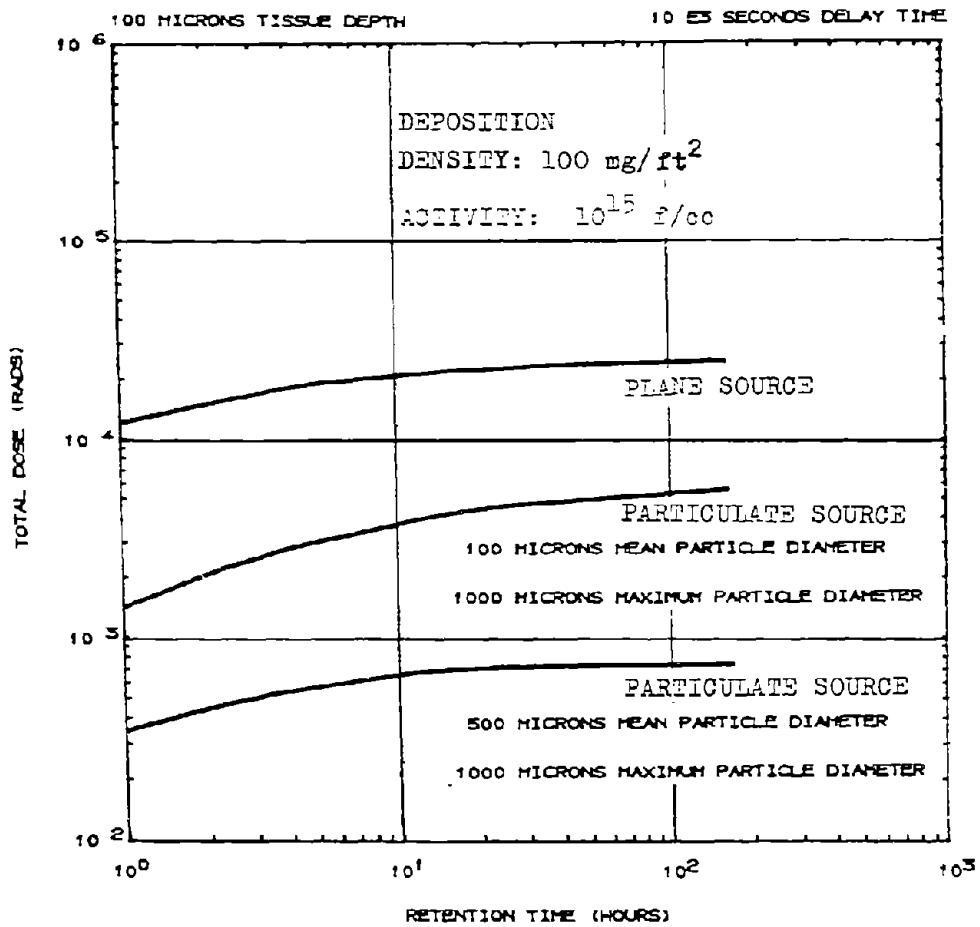


Figure 6
Comparison between Doses Computed for a
Plane Source and the Corresponding
Values for a Multiparticle Source

VIII. DOSE CRITERIA FOR MULTIPLE-PARTICLE DEPOSITION

To date no criterion has been explicitly proposed for skin damage from multiple particles. However, the following points serve as guidelines for establishing such a criterion:

1. As in the case of single-particle sources, damage to the skin will occur when the survival level of the germinative cells is reduced to less than 0.001 over an area sufficiently large to preclude replacement of dead cells via proliferation.⁽¹⁷⁾

2. Such a reduction in survival occurs at a lower dose level from a multiparticle source than it would from a single particle. Krebs estimates that a uniform 1300-rad dose from a multiparticle source would cause the same reduction in survival level brought about by a 1500-rad dose from a single-particle source.⁽²⁰⁾

3. In view of the difference between the predicted single-particle critical dose (1500 rad) and the corresponding experimentally determined value of 660 rads, an adjustment has to be made to the suggested multiple-particle value to bring it into line with experiment.

4. It seems reasonable to accept a proportional dose for the multi-particle situation; i.e. $(1300/1500) \times 660 \sim 570$ rads. That is, exposure of the skin (100 μ depth) to a uniform deposited dose of 570 rad from a multiple source will be assumed sufficient to damage the skin in the manner described in Section VI above.

III. RESULTS AND DISCUSSION

A. Beta Doses From Single particles

1. Particles Containing Unfractionated Fission-Product Mixtures

Point depth doses (estimated at 100μ tissue depth directly below the fallout particle) and Krebs doses (estimated at a point radially displaced 4000μ in a plane 100μ below the skin surface) were computed for particles 50, 100, 200, 500, 750 and 1000μ in diameter; for each particle size, doses were computed for 10^3 , 10^4 , 10^5 and 10^6 seconds of delay time (time between weapon detonation and deposition of the particle on the skin). The fallout particles were assumed to contain 10^{15} fissions per cubic centimeter. For all but exceptional situations, 10^{15} fissions/cc is considered the maximum expected fallout activity. Beta doses from fallout of higher fission density can be obtained, by linear extrapolation, from the values reported here.

Figures 7 to 14 are presentations of the computer-plotted doses as functions of particle retention time on the skin. It can be seen from Figure 7, which presents Krebs doses for the earliest particle arrival time considered, that single fallout particles smaller than 500μ in diameter, landing on the skin as early as 10^3 seconds (16.7 min.) after detonation, will not cause any skin burns. A single 500μ particle arriving even this early has to be retained about 10 hours before it delivers the 660 rads required for damage. Table 5 shows experimental data obtained at Oak Ridge National Laboratory (ORNL) for expected retention times of particles on human skin under normal conditions of temperature and humidity⁽²¹⁾. Considering the values in Table 5, it is obvious that even a 500μ particle would be incapable of producing a 1 mm lesion.

KREBS DOSE VERSUS RETENTION TIME

10²³ SECONDS DELAY TIME

100 MICRONS TISSUE DEPTH

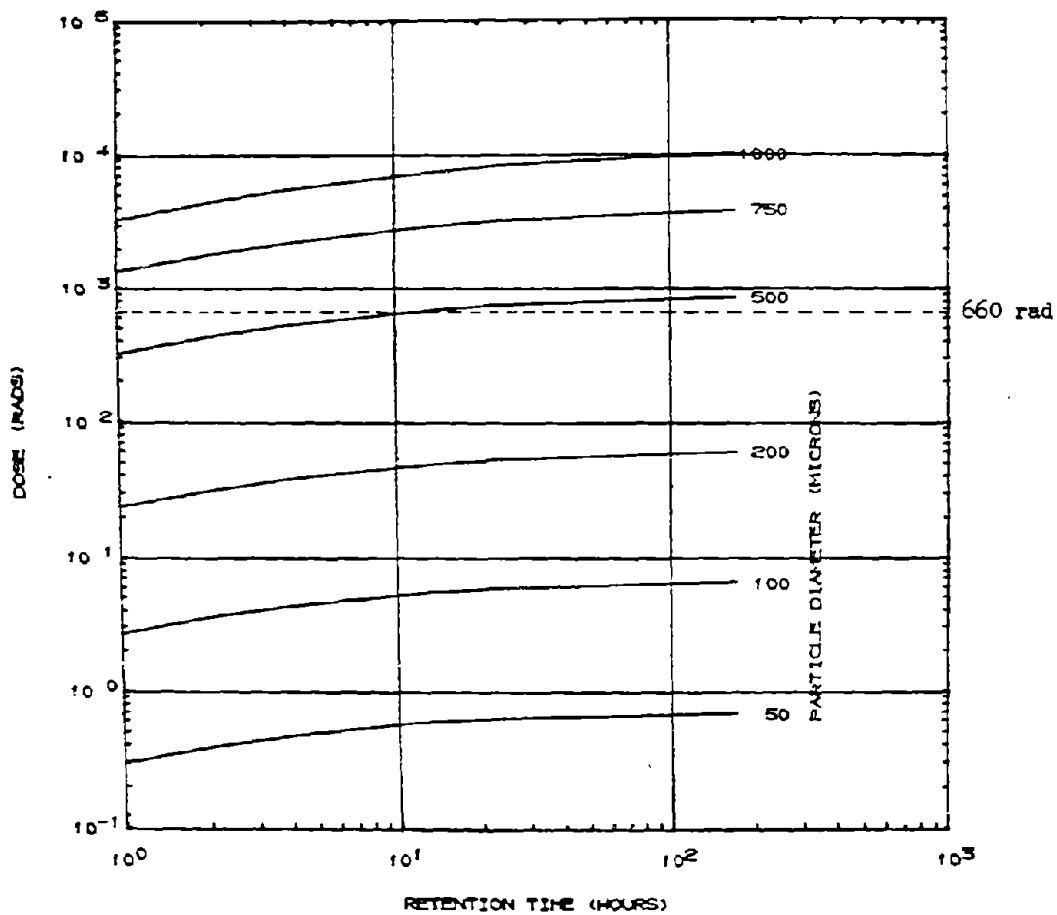


Figure 7
Krebs Dose Delivered to the Skin
by Single Fallout Particles

POINT DEPTH DOSE VERSUS RETENTION TIME

10²³ SECONDS DELAY TIME

100 MICRONS TISSUE DEPTH

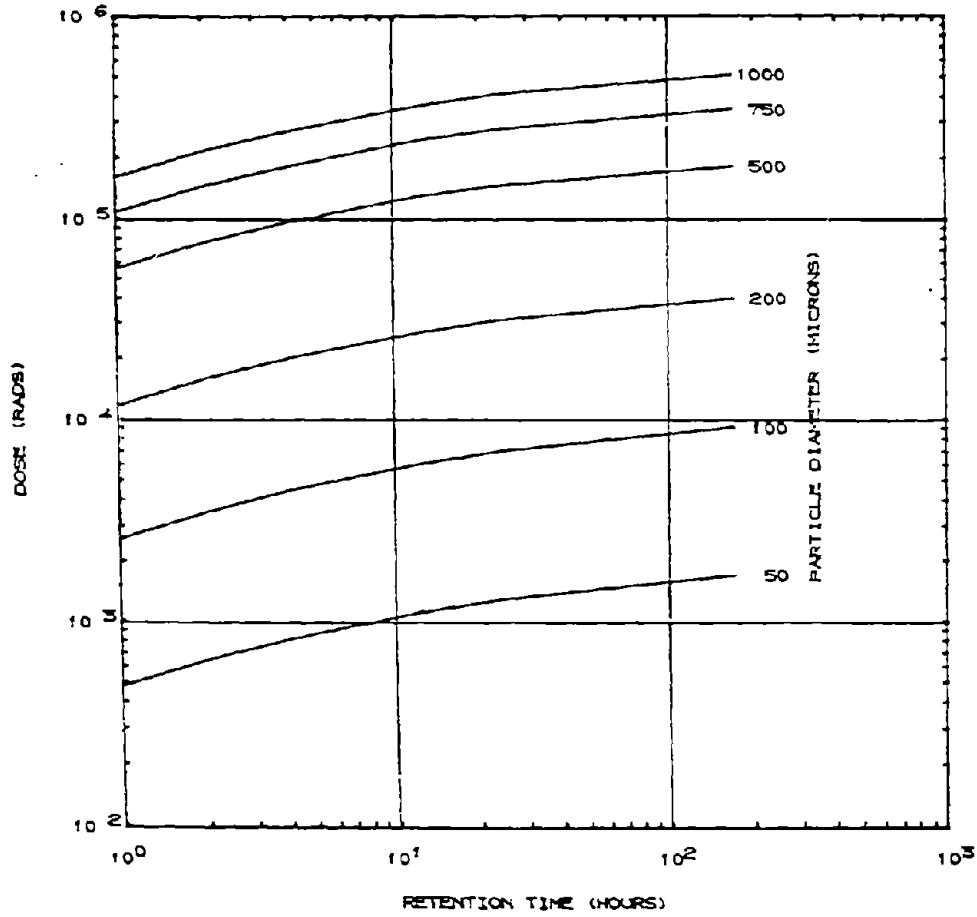


Figure 8
Point Depth Dose Delivered to the Skin
by Single Fallout Particles

KREBS DOSE VERSUS RETENTION TIME

10 24 SECONDS DELAY TIME

100 MICRONS TISSUE DEPTH

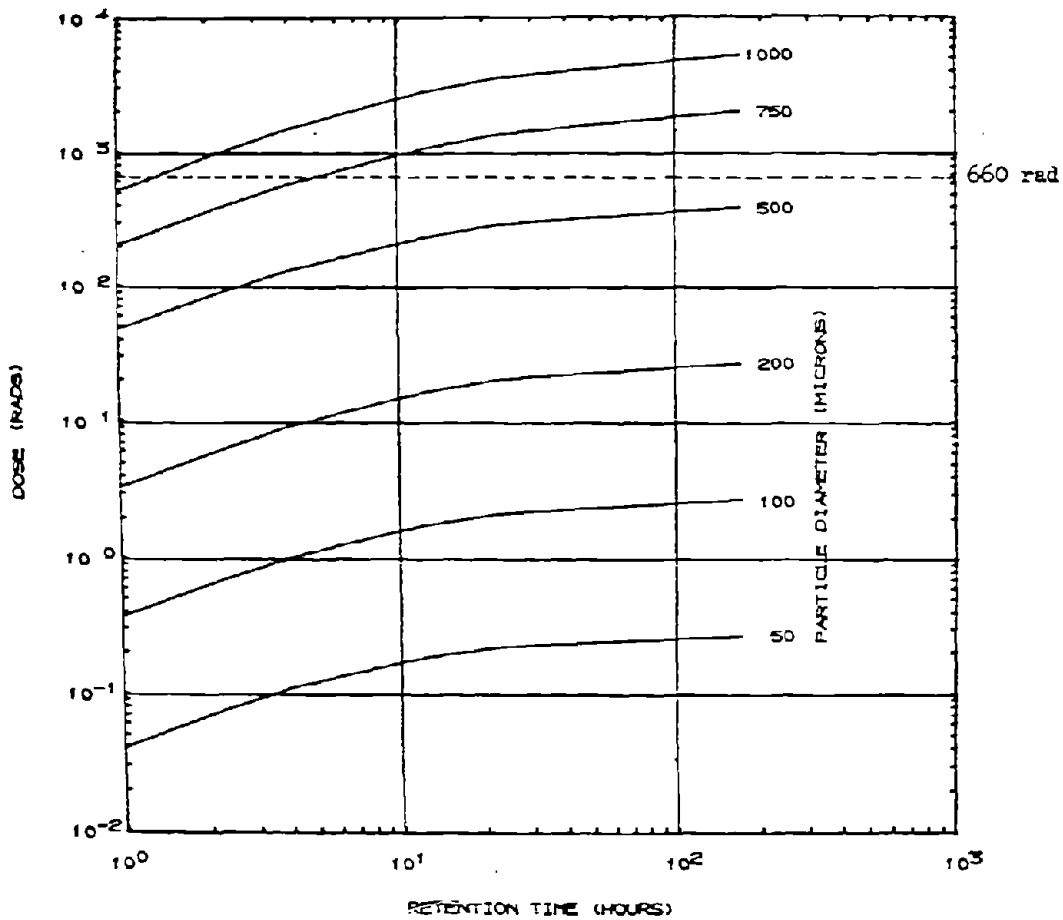


Figure 9
Krebs Dose Delivered to the Skin
by Single Fallout Particles

POINT DEPTH DOSE VERSUS RETENTION TIME

10²⁴ SECONDS DELAY TIME

100 MICRONS TISSUE DEPTH

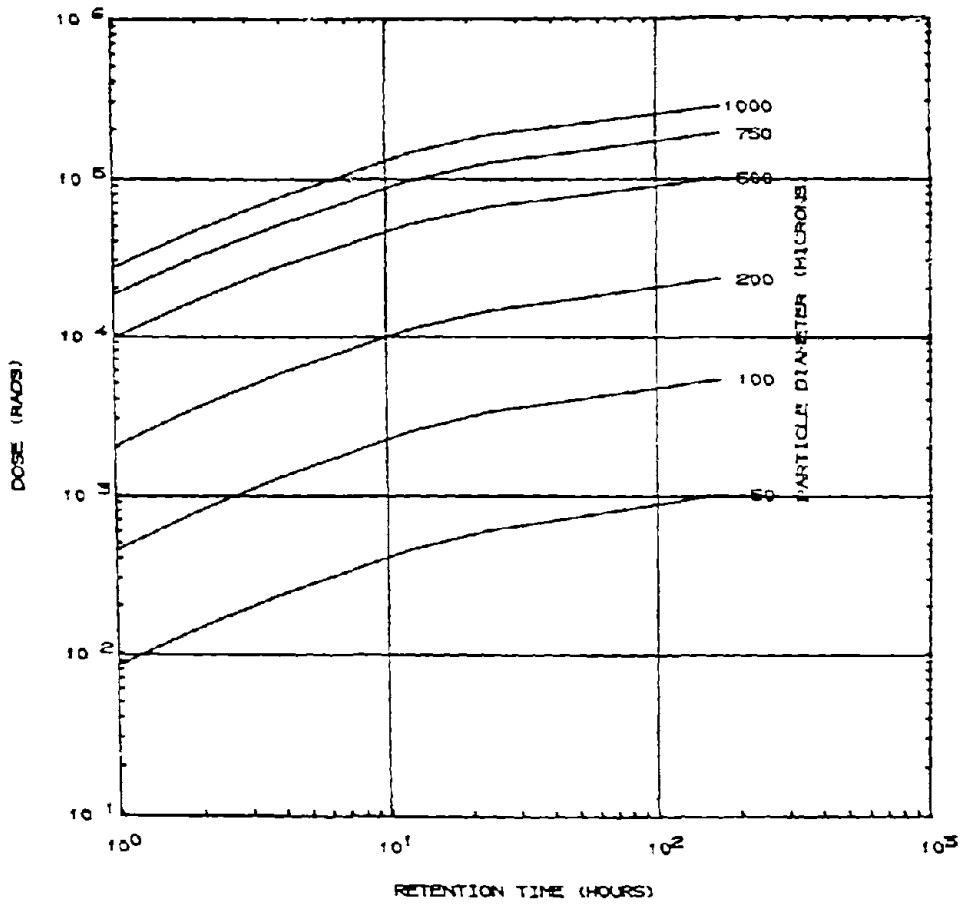


Figure 10

Point Depth Dose Delivered to the
Skin by Single Fallout Particles

KREBS DOSE VERSUS RETENTION TIME

10 EB SECONDS DELAY TIME

100 MICRONS TISSUE DEPTH

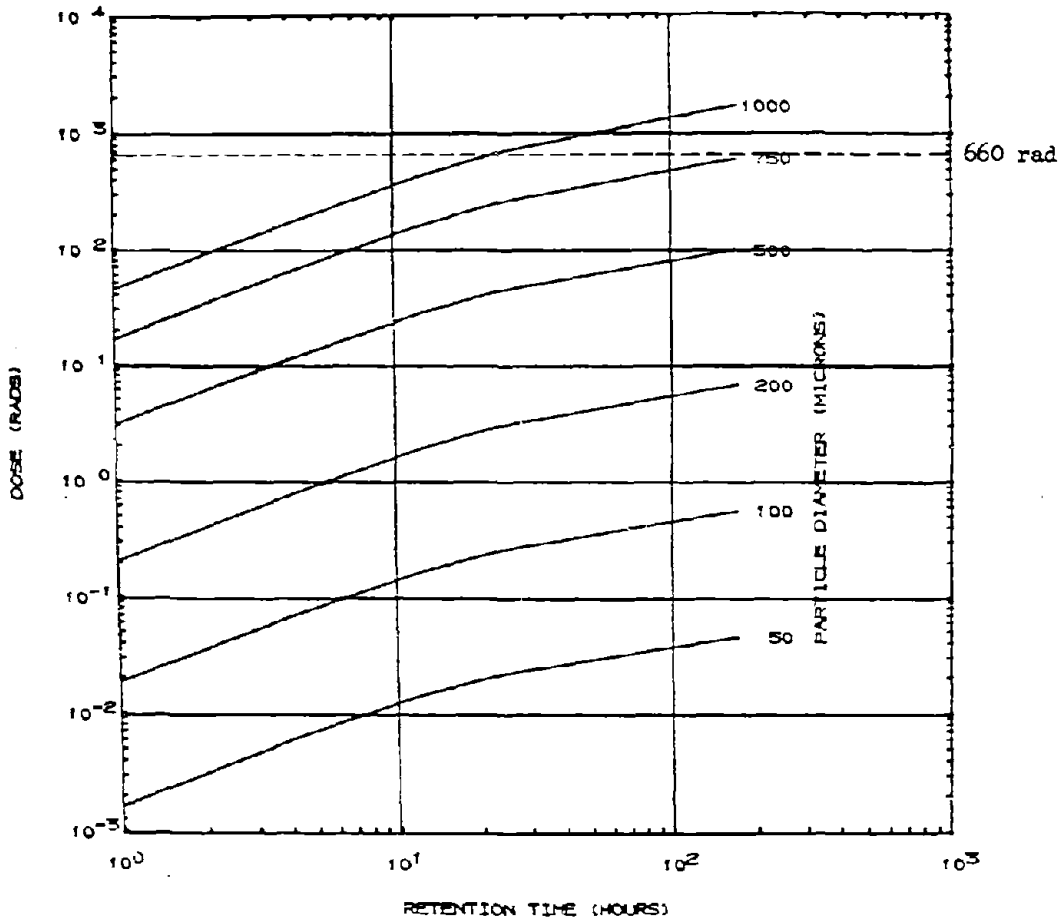


Figure 11
Krebs Dose Delivered to the Skin
by Single Fallout Particles

POINT DEPTH DOSE VERSUS RETENTION TIME

10²⁵ SECONDS DELAY TIME

100 MICRONS TISSUE DEPTH

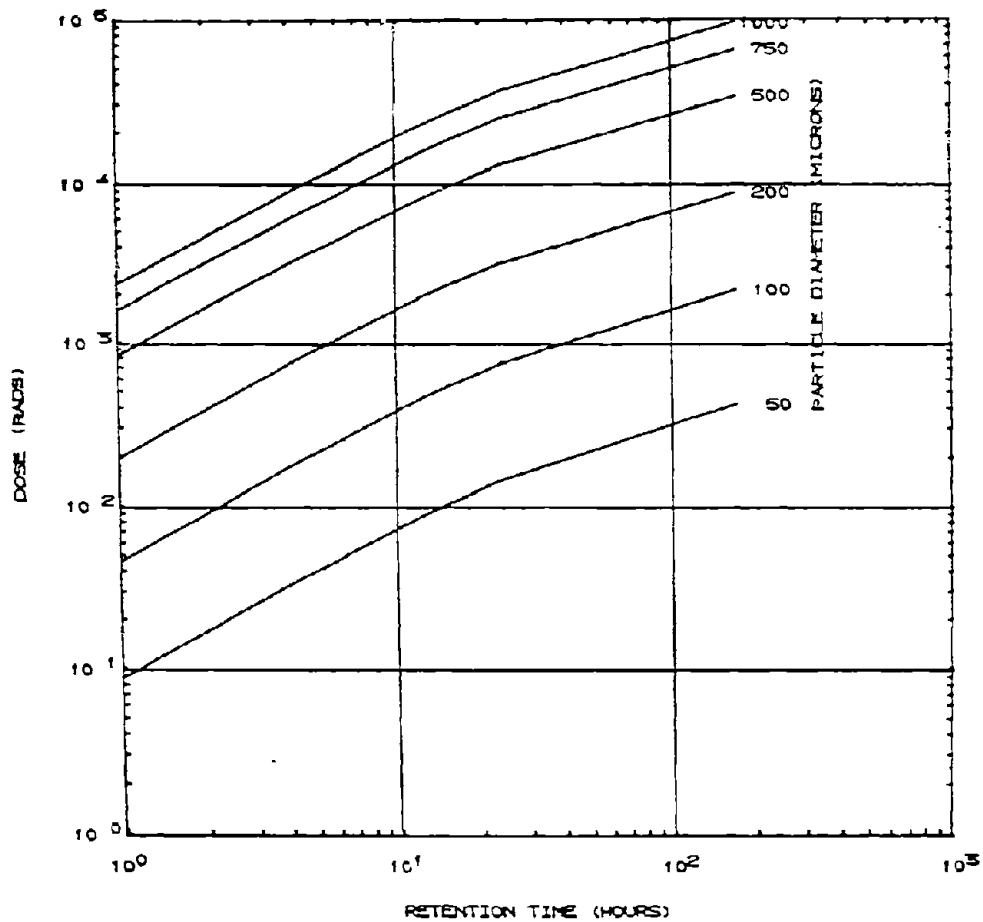


Figure 12

Point Depth Dose Delivered to the
Skin by Single Fallout Particles

KREBS DOSE VERSUS RETENTION TIME

10 EA SECONDS DELAY TIME

100 MICRONS TISSUE DEPTH

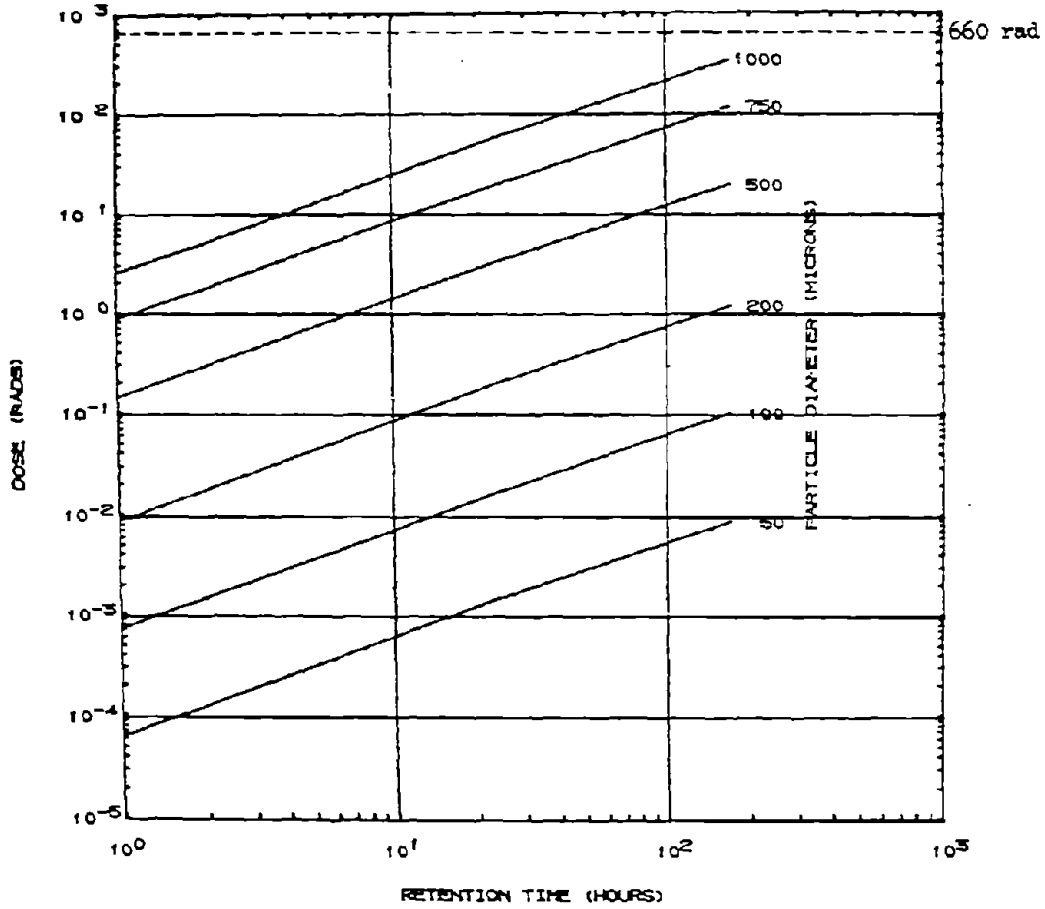


Figure 13
Krebs Dose Delivered to the Skin
by Single Fallout Particles

POINT DEPTH DOSE VERSUS RETENTION TIME

10 26 SECONDS DELAY TIME

100 MICRONS TISSUE DEPTH

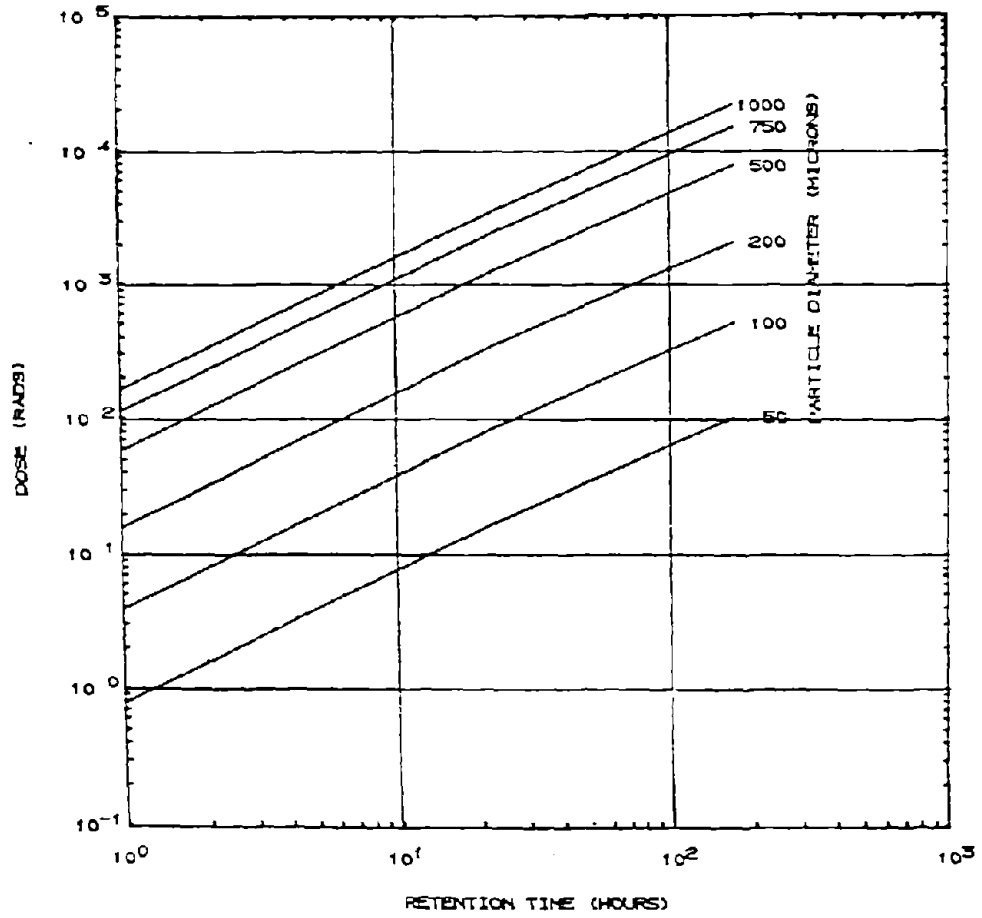


Figure 14

Point Depth Dose Delivered to the Skin by Single Fallout Particles

TABLE 5

EXPECTED RETENTION TIMES OF PARTICLES ON HUMAN SKIN*

<u>Particle Diameter, μ</u>	<u>Time, Hours</u>
50	6.8
100	3.5
200	2.7
500	2.2
750	2.1
1000	2.0

*From Reference 21

Figure 8 presents the point depth doses delivered by the same particles under the same (early arrival) conditions. Comparison between Figures 7 and 8 shows that point depth doses are higher than the corresponding Krebs doses by a factor of 10^2 to 10^3 , depending on the particle size. Lower ratios correspond to larger particle sizes.

From Figures 9 and 11, it can be seen that, after a delay of a little over 10^4 seconds (about 2.8 hours), even a 1000μ particle can be tolerated, provided its retention time does not exceed its expected value in Table 5.

Figure 11 shows further that, after a delay of 10^5 seconds (about 28 hours), no single particle of any size can possibly cause a beta burn (except for the 1000μ particle retained for an inordinately long time).

2. Particles Containing Fractionated Fission-Product Mixtures

The objective of this Section is to determine the magnitude of the effect of fractionation on the beta doses delivered by fallout particles rather than to obtain a set of beta-dose values from particles containing fractionated fission-product mixtures. Therefore, the calculations were limited to four fallout-particle sizes, one device (5 Mt), one theory of charge distribution* (Glendenin's), one delay time (one hour), and one exposure period (24 hours). Three values of the fractionation ratio ($r_{89,95} = 0.333, 0.1$ and 0.01) were postulated, however, to permit investigation of the effect of that parameter on the doses.

Table 6 contains the F_R values calculated by Freiling⁽¹⁰⁾ for the significant mass chains in the case under consideration. As previously mentioned, the same F_R value was used for all the members of a given mass chain.

* See Section IV.

TABLE 6

Fraction of Atoms (F_R) That Exist in the Form
of Refractory Elements at the Time of Solidification
(From Reference 10)

Solidification Temperature: 1400 °C

Solidification Time: 41 sec post detonation (5 Mt)

CHAIN	F_R	CHAIN	F_R	CHAIN	F_R
83	0.00	105	0.80	141	0.96
84	0.00	106	0.95	142	1.00
85	0.00	107	0.99	143	1.00
87	0.00	118	1.00	144	1.00
88	0.00	125	1.00	145	1.00
89	0.00	126	1.00	146	1.00
90	0.08	127	1.00	147	1.00
91	0.17	128	1.00	149	1.00
92	0.83	129	0.98	151	1.00
93	0.99	131	0.84	152	1.00
94	0.99	132	0.58	155	1.00
95	1.00	133	0.50		
97	1.00	134	0.02		
98	1.00	135	0.00		
99	0.83	137	0.00		
101	0.07	138	0.00		
102	0.01	039	0.06		
103	0.17	140	0.32		

Table 7 gives the calculated point depth doses and Krebs doses from unfractionated and fractionated sources, while Table 8 depicts the ratios of fractionated to their corresponding unfractionated doses. As can be seen from the Table, the ratios for point depth doses varied from about 0.70 to 0.47, and for Krebs doses from about 0.75 to 0.50, indicating that even in extreme cases of fractionation, doses from fractionated sources are lower by a factor of only 2 than those from unfractionated sources. Although a factor of 2 might be significant in certain cases, yet due to the uncertainties in the assumptions involved in the complex computations, further calculations or refinements did not seem justified.

B. Gamma Doses from Single Particles

In this Section, the goal is to obtain a rough estimate of the contribution of the gamma dose relative to the beta dose at the germinal-layer level. The gamma-dose to beta-dose ratio is naturally affected by several parameters, including particle size, tissue depth, position of point of interest at which dose is to be estimated, delay time, exposure time, and fractionation. An adequate idea can, however, be obtained from a limited amount of computation.

Calculations were made for one particle size (100μ in diameter), one tissue depth (100μ), one point in tissue (directly below the particle), and an unfractionated fission-product mixture. Several delay and exposure times were considered, however.

Results of the calculations are presented in Table 9. They cover delay times ranging from 10^3 to 10^5 seconds and exposure times from 1200 seconds to infinity.

TABLE 7

Beta Doses (Rads) From Fallout Particles Containing
Unfractionated and Fractionated Fission-Product Mixtures

Fission Density: 10^{15} fissions/cm³
 Delay Time: 1 hr
 Exposure Time: 24 hr

Particle Size μ	Unfractionated		Fractionated					
	Point* Depth	Krebs	R** = 0.333		R** = 0.1		R** = 0.01	
50	1.09×10^3	4.25×10^{-1}	Point* Depth	Krebs	Point* Depth	Krebs	Point* Depth	Krebs
100	5.84×10^3	3.96×10^0	7.58×10^2	3.19×10^{-1}	6.06×10^2	2.71×10^{-1}	5.04×10^2	2.39×10^{-1}
200	2.68×10^4	3.88×10^1	4.03×10^3	2.95×10^0	3.21×10^3	2.49×10^0	2.67×10^3	2.18×10^0
500	1.34×10^5	7.13×10^2	1.86×10^4	2.84×10^1	1.49×10^4	2.37×10^1	1.24×10^4	2.05×10^1
			9.34×10^4	5.12×10^2	7.52×10^4	4.21×10^2	6.32×10^4	3.60×10^2

* Point Depth dose at 100μ below the skin surface

**R = 89, 95, the Fractionation Ratio

TABLE 8

Ratio of Beta Doses from Particles Containing Fractionated Fission-Product Mixtures to Beta Doses from Particles Containing Unfractionated Mixtures

Fission Density: 10^{15} fissions/cm³
 Delay Time: 1 hr
 Exposure Time: 24 hr

Parti- cle Size μ	DOSE RATIOS							
	R = 0.333		R = 0.1		R = 0.01		R = 0.01	
	Point Depth	Krebs	Point Depth	Krebs	Point Depth	Krebs	Point Depth	Krebs
50	0.695	0.751	0.556	0.638	0.462	0.562	0.462	0.562
100	0.690	0.745	0.550	0.629	0.457	0.550	0.457	0.550
200	0.694	0.732	0.556	0.611	0.463	0.528	0.463	0.528
500	0.697	0.718	0.561	0.591	0.472	0.505	0.472	0.505

TABLE 9

Gamma Doses from Fallout Particles

Fission Density: 10^{15} f/cm³
 Particle Diameter: 100 μ
 Tissue Depth: 100 μ (Point Depth Dose, Rad)

A		1200 sec	1 hr	2 hrs	4 hrs	6 hrs	12 hrs	18 hrs	24 hrs	168 hrs	∞
B	10^3 sec	6.32×10^{-1}	1.28×10^2	1.73×10^2	2.14×10^2	2.35×10^2	2.66×10^2	2.83×10^2	2.93×10^2	3.43×10^2	4.10×10^2
	1 hr	2.46×10^{-1}	5.70×10^1	8.58×10^1	1.16×10^2	1.33×10^2	1.62×10^2	1.78×10^2	1.88×10^2	2.36×10^2	3.03×10^2
	2 hrs	1.14×10^{-1}	2.88×10^1	4.68×10^1	6.89×10^1	8.29×10^1	1.08×10^2	1.22×10^2	1.32×10^2	1.79×10^2	2.47×10^2
	10^4 sec	7.56×10^0	1.98×10^1	3.33×10^1	5.13×10^1	6.36×10^1	8.67×10^1	1.00×10^2	1.09×10^2	1.56×10^2	2.23×10^2
	4 hrs	4.65×10^0	1.26×10^1	2.21×10^1	3.61×10^1	4.64×10^1	6.68×10^1	7.93×10^1	8.77×10^1	1.33×10^2	2.00×10^2
	6 hrs	2.72×10^0	7.63×10^0	1.40×10^1	2.43×10^1	3.24×10^1	4.95×10^1	6.03×10^1	6.79×10^1	1.11×10^2	1.78×10^2
	12 hrs	1.20×10^0	3.49×10^0	6.66×10^0	1.22×10^1	1.70×10^1	2.79×10^1	3.54×10^1	4.11×10^1	7.92×10^1	1.45×10^2
	18 hrs	7.26×10^{-1}	2.13×10^0	4.11×10^0	7.69×10^0	1.09×10^1	1.84×10^1	2.41×10^1	2.85×10^1	6.30×10^1	1.28×10^2
	24 hrs	4.91×10^{-1}	1.44×10^0	2.81×10^0	5.32×10^0	7.59×10^0	1.32×10^1	1.76×10^1	2.12×10^1	5.28×10^1	1.17×10^2
	10^5 sec	3.98×10^{-1}	1.17×10^0	2.29×10^0	4.37×10^0	6.26×10^0	1.11×10^1	1.49×10^1	1.81×10^1	4.82×10^1	1.12×10^2

A: Exposure Time

B: Delay Time

A direct comparison between beta- and gamma-dose contributions to the total skin exposure can be made from Figure 15, in which both types of dose are shown as functions of exposure time. It is clear that there is more than an order-of-magnitude difference between the values of the two doses for the particle size examined. Thus, for 100μ particles, the gamma-dose contribution to skin damage appears to be negligible. It is certain, however, that as the particle size increases, the β/γ ratio decreases due to the high absorption and scattering of the betas within the body of the particle itself, relative to the gammas. For a better definition of the effect of size on the β/γ ratio, more computations would have to be carried out.

C. Beta Doses From Multiparticle Fallout

Data computed with the Multiparticle Model are shown in Figures 16 to 40. In these figures, time-integrated doses from fallout deposition densities of 100, 200, 500, 1000, 2000 and 5000 mg/ft^2 , for different particle-size distributions, have been plotted as functions of fallout retention time. All computations are based on 10^{15} fissions/cc. Delay times of 10^3 , 10^4 , 10^5 , 10^6 and 10^7 seconds are covered.

Figure 16 shows that for a delay time of 10^3 seconds even the lowest deposition density ($100 \text{ mg}/\text{ft}^2$) of particles of 100μ mean diameter and 1000μ maximum diameter (size distribution A), can deliver to the skin, in less than one hour, more than the 570 rads required for damage in the multiparticle situation. However, as seen in Figure 20, the same mass of fallout but of 1000μ mean diameter and 2000μ maximum diameter

Fission Density = 10^{15} f/cm³

100 MICRONS TISSUE DEPTH

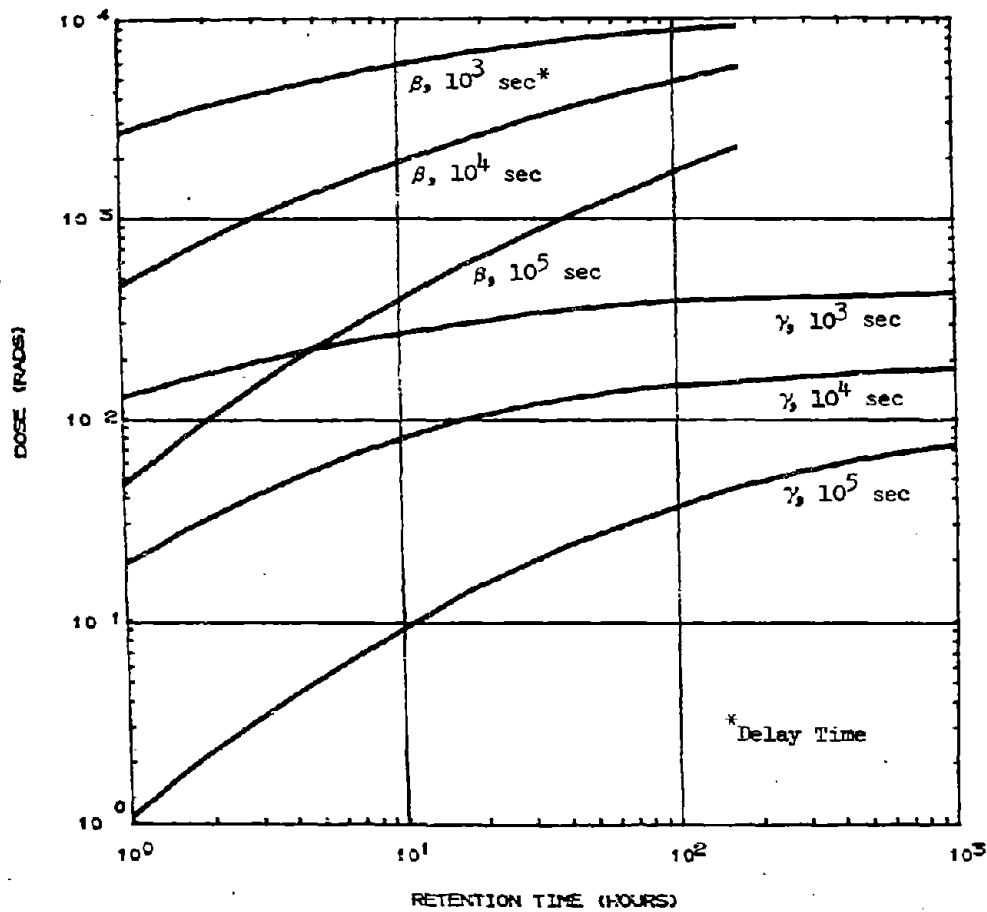


Figure 15
Point Depth Beta and Gamma
Dose from a 100 μ Particle

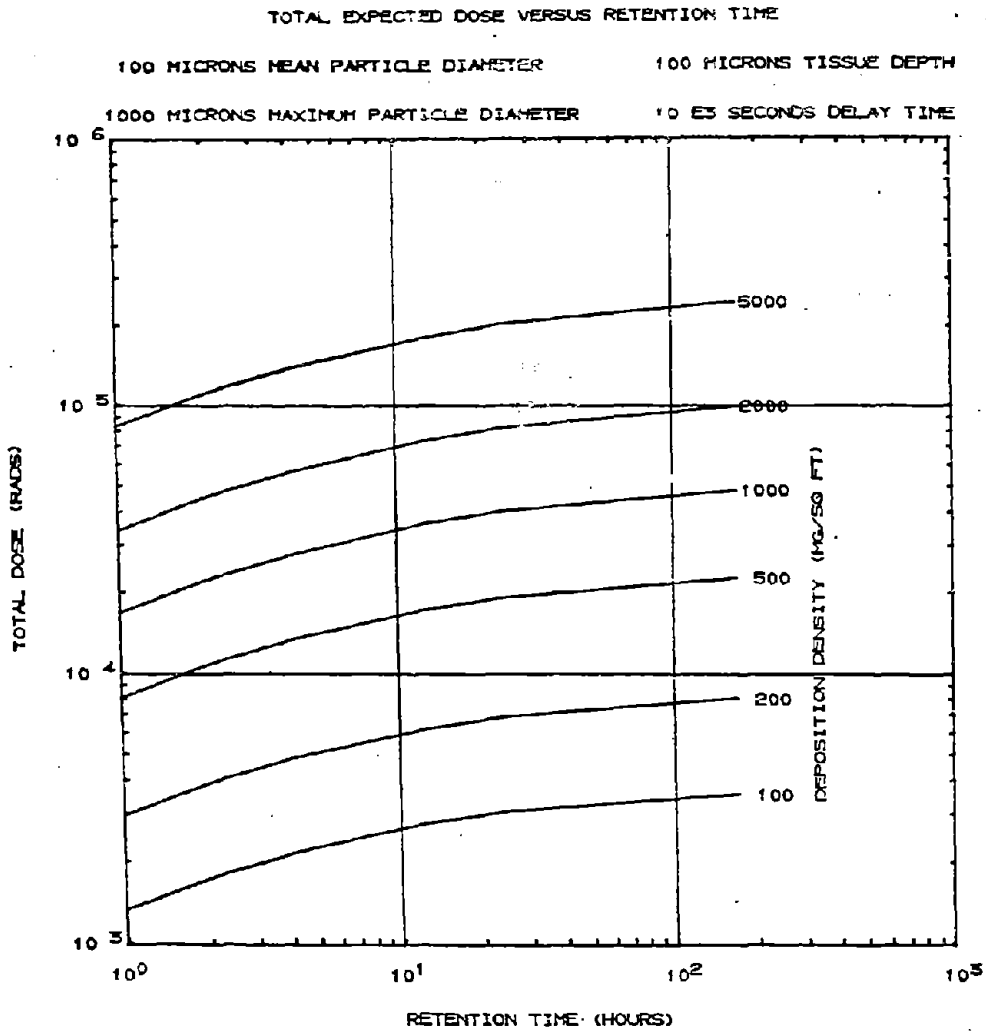


Figure 16
Beta Dose Delivered to the
Skin by Multiparticle Fallout

TOTAL EXPECTED DOSE VERSUS RETENTION TIME

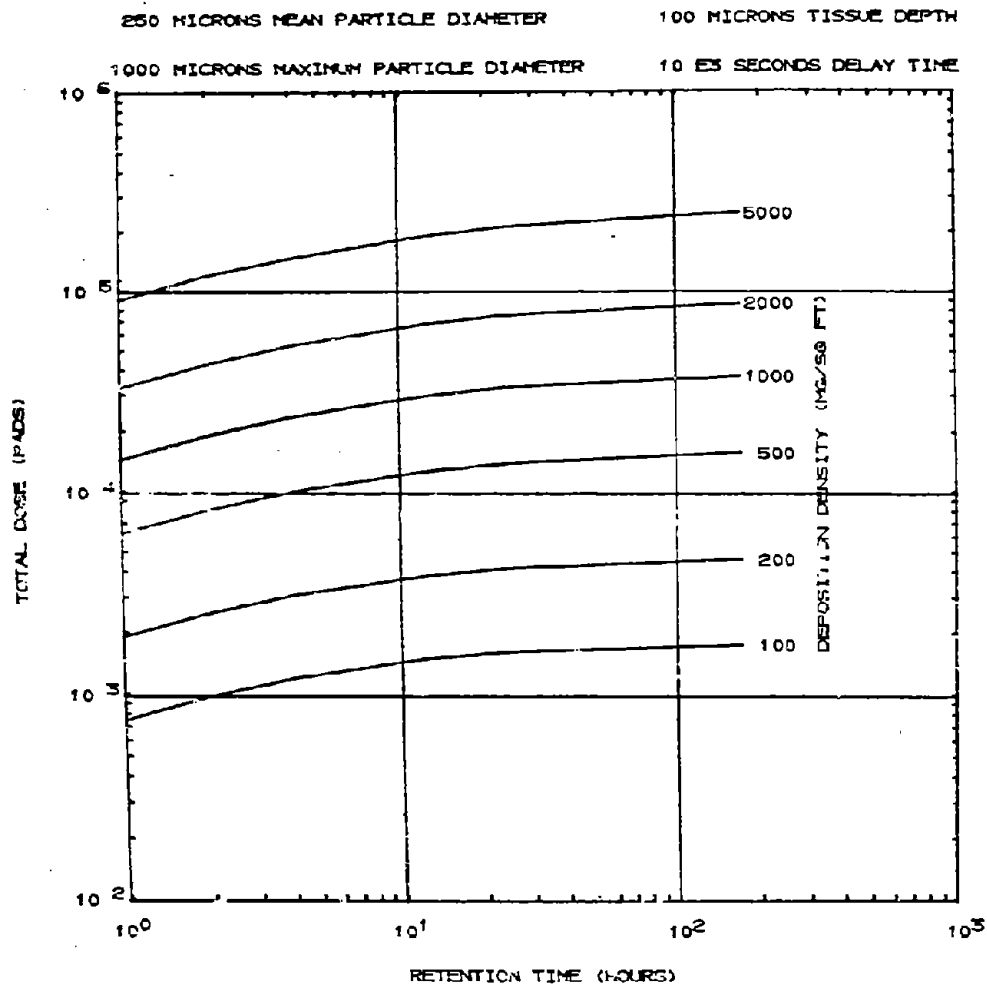


Figure 17
Beta Dose Delivered to the
Skin by Multiparticle Fallout

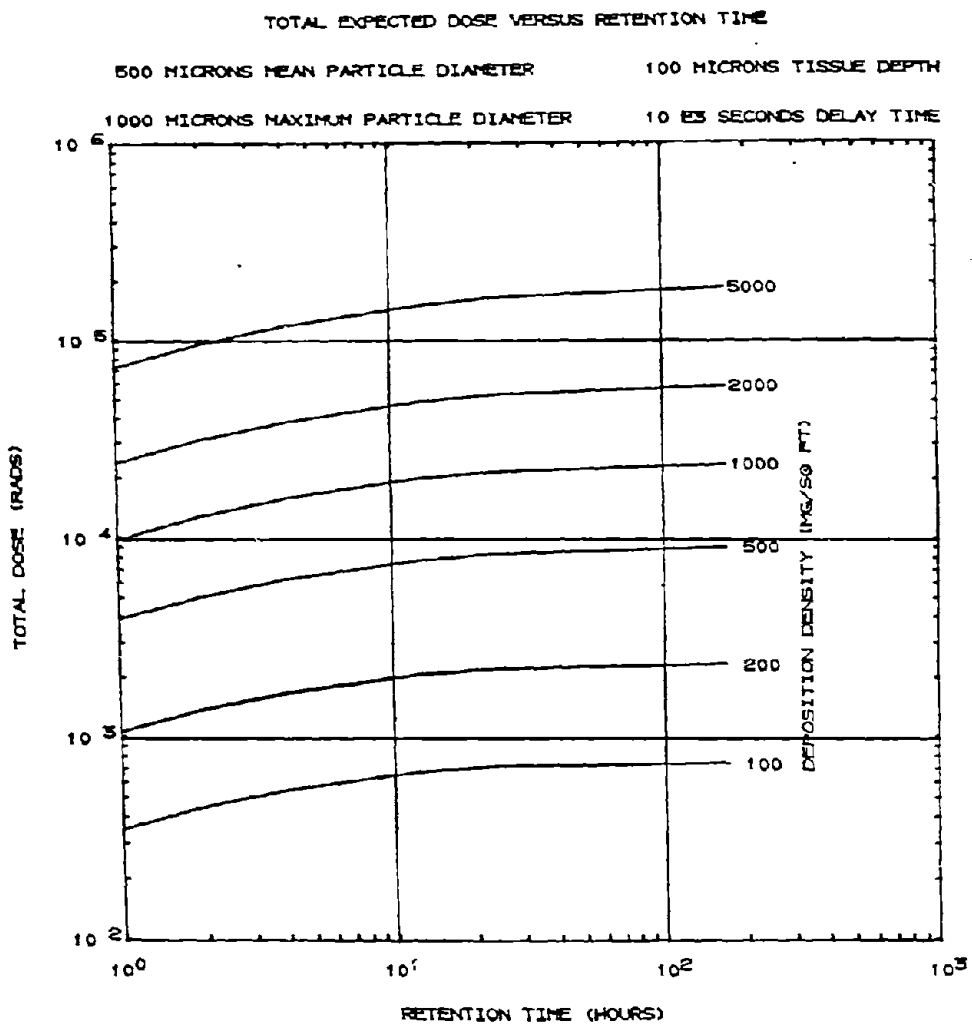


Figure 18
Beta Dose Delivered to the
Skin by Multiparticle Fallout

TOTAL EXPECTED DOSE VERSUS RETENTION TIME

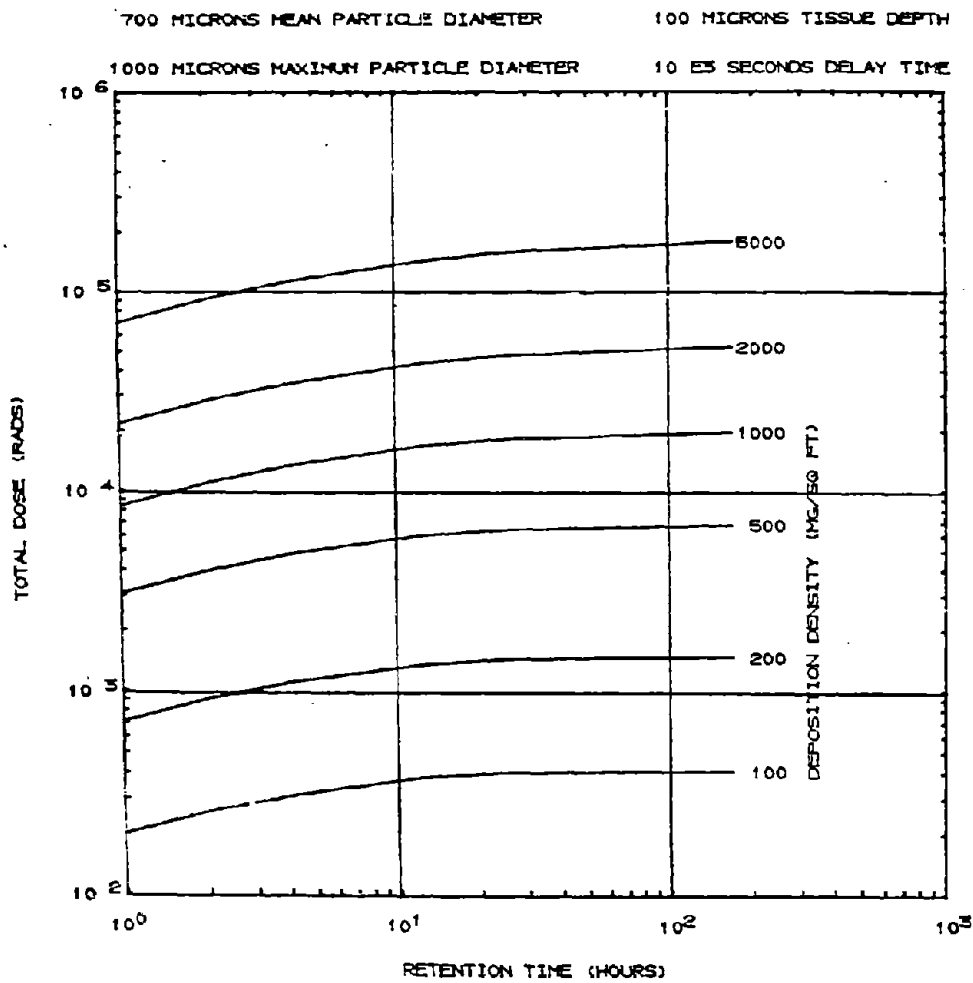


Figure 19
 Beta Dose Delivered to the
 Skin by Multiparticle Fallout

TOTAL EXPECTED DOSE VERSUS RETENTION TIME

1000 MICRONS MEAN PARTICLE DIAMETER

100 MICRONS TISSUE DEPTH

2000 MICRONS MAXIMUM PARTICLE DIAMETER

10²³ SECONDS DELAY TIME

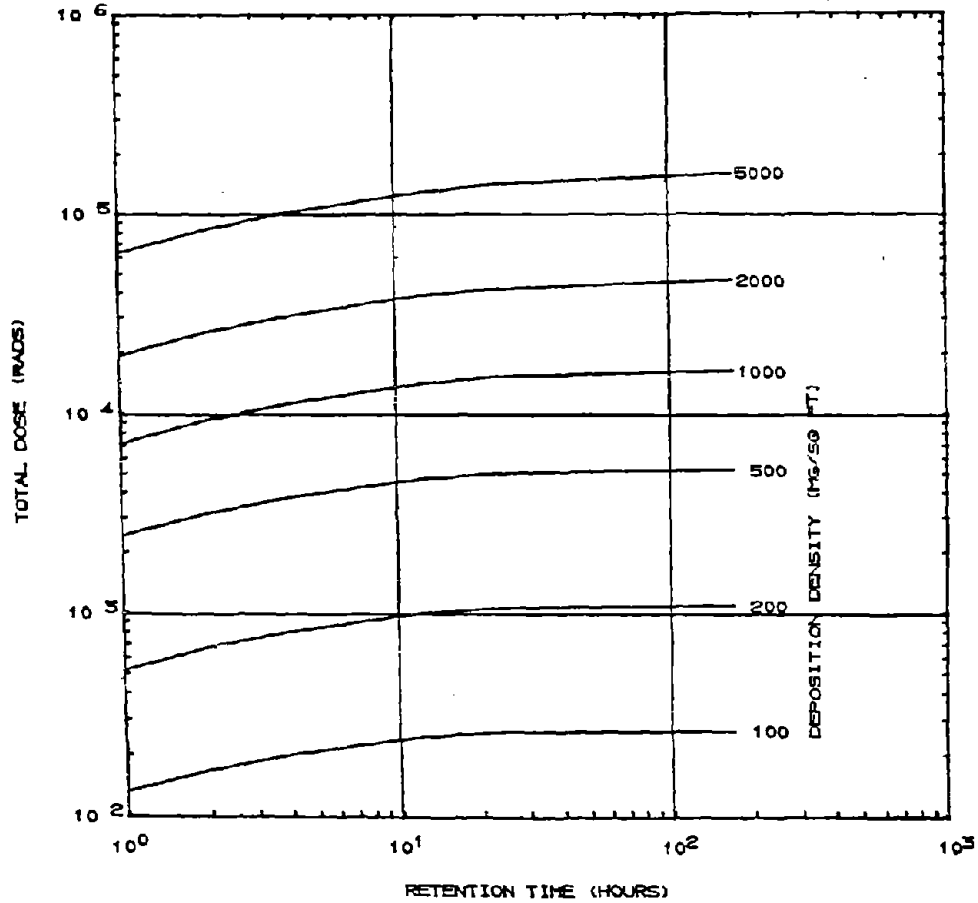


Figure 20

Beta Dose Delivered to the
Skin by Multiparticle Fallout

TOTAL EXPECTED DOSE VERSUS RETENTION TIME

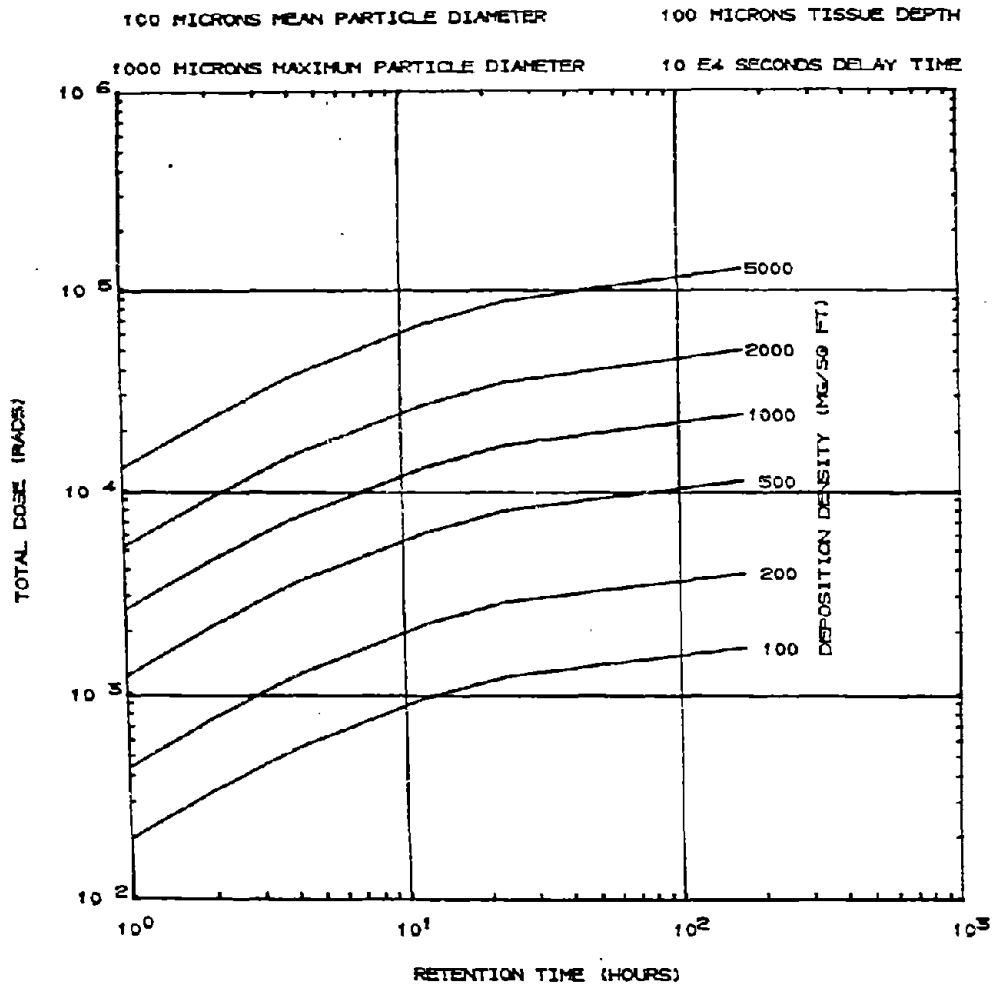


Figure 21
 Beta Dose Delivered to the
 Skin by Multiparticle Fallout

TOTAL EXPECTED DOSE VERSUS RETENTION TIME

250 MICRONS MEAN PARTICLE DIAMETER

100 MICRONS TISSUE DEPTH

1000 MICRONS MAXIMUM PARTICLE DIAMETER

10 E4 SECONDS DELAY TIME

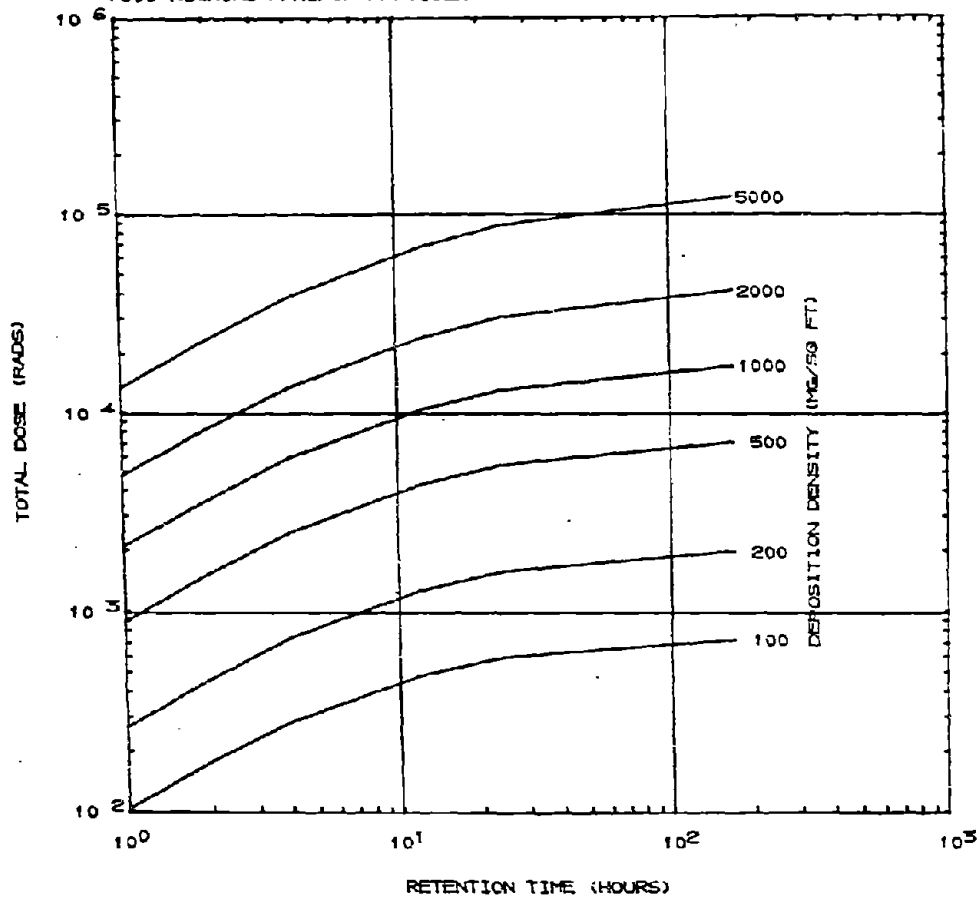


Figure 22

Beta Dose Delivered to the Skin by Multiparticle Fallout

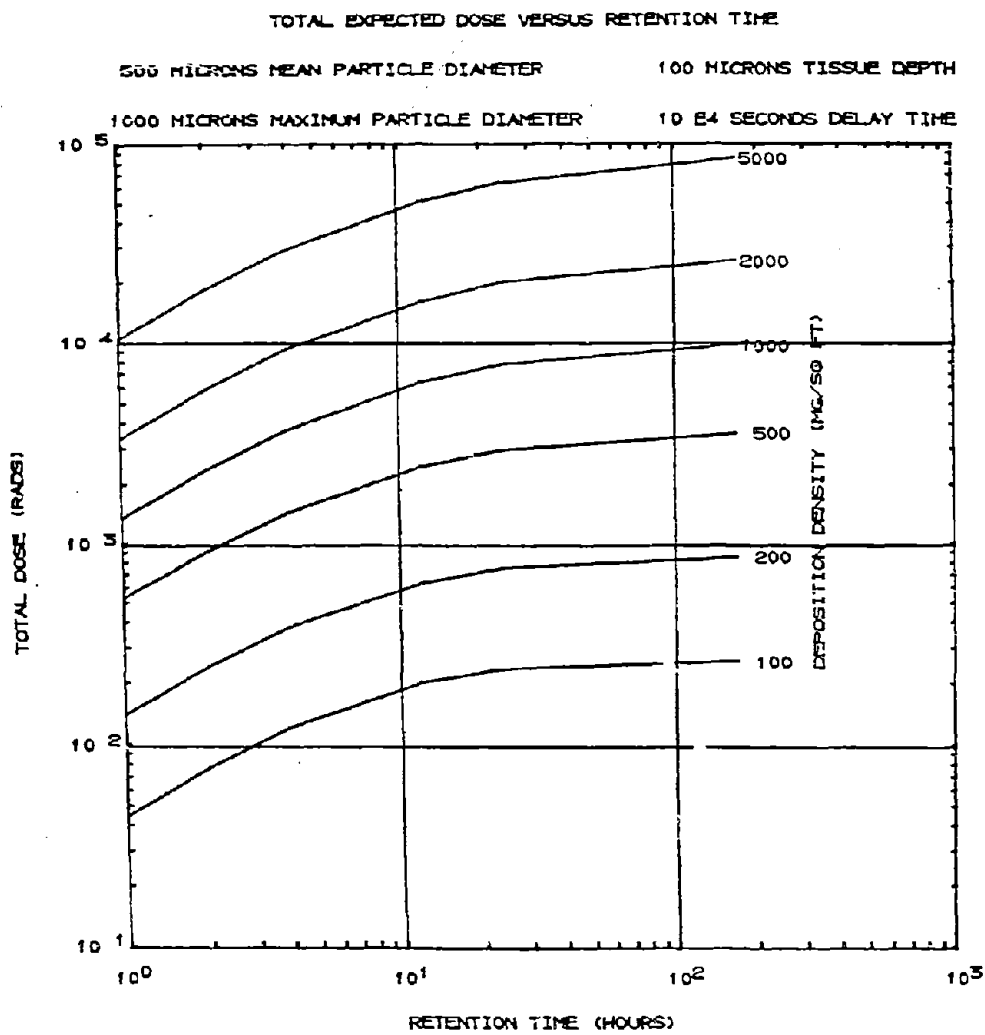


Figure 23
Beta Dose Delivered to the
Skin by Multiparticle Fallout

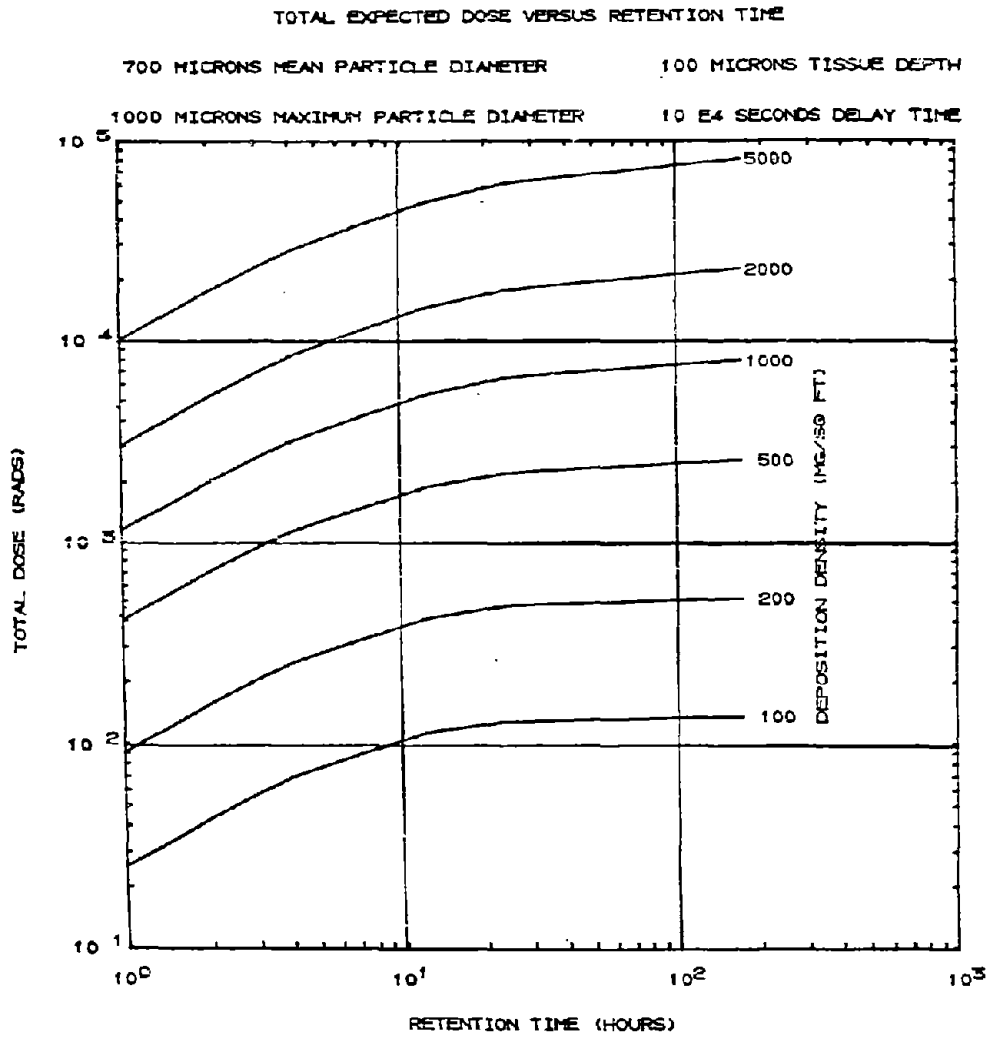


Figure 24
Beta Dose Delivered to the
Skin by Multiparticle Fallout

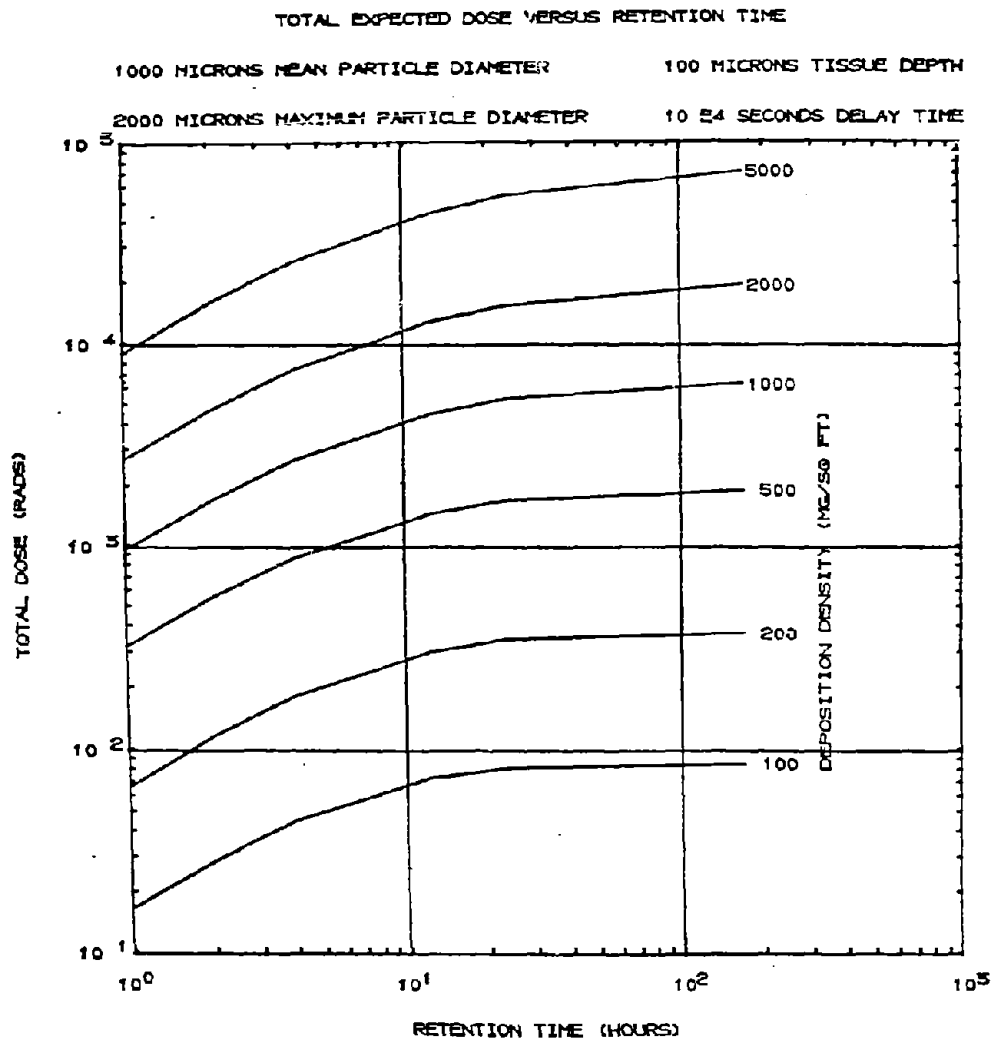


Figure 25
Beta Dose Delivered to the
Skin by Multiparticle Fallout

TOTAL EXPECTED DOSE VERSUS RETENTION TIME

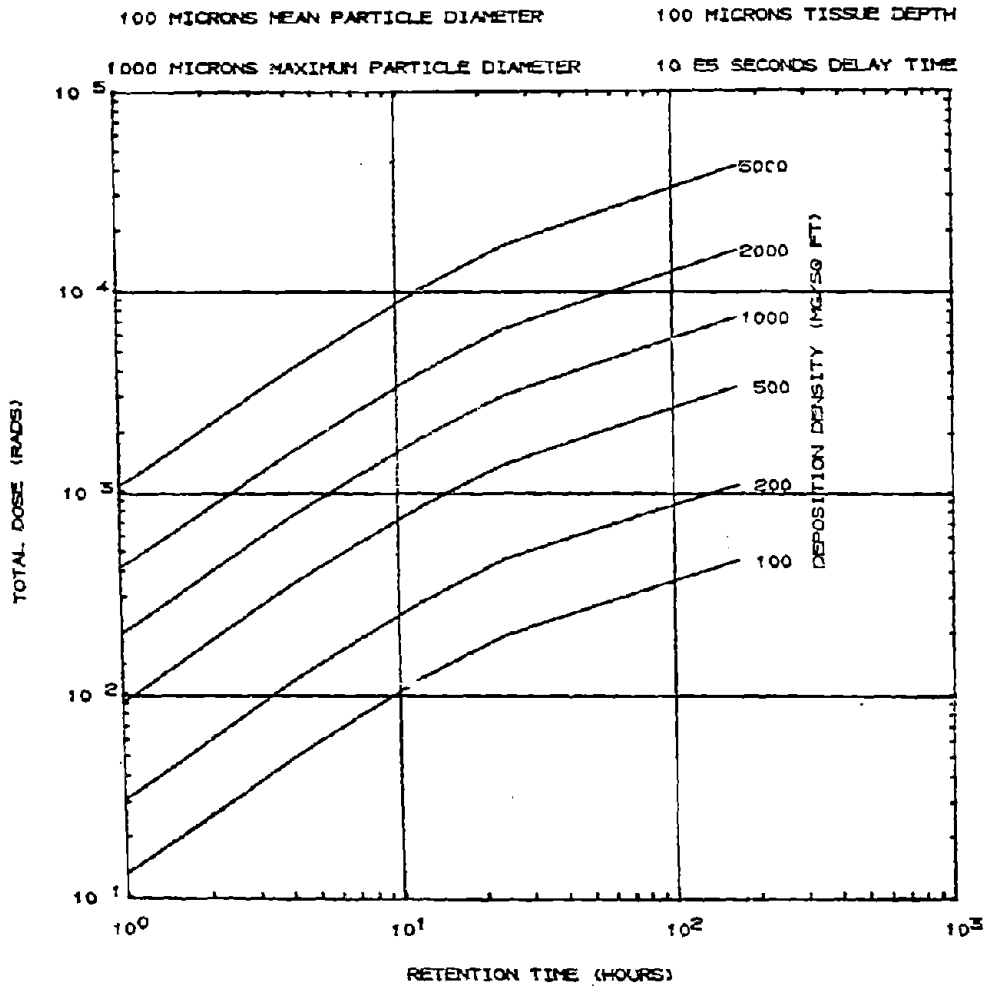


Figure 26

Beta Dose Delivered to the
Skin by Multiparticle Fallout

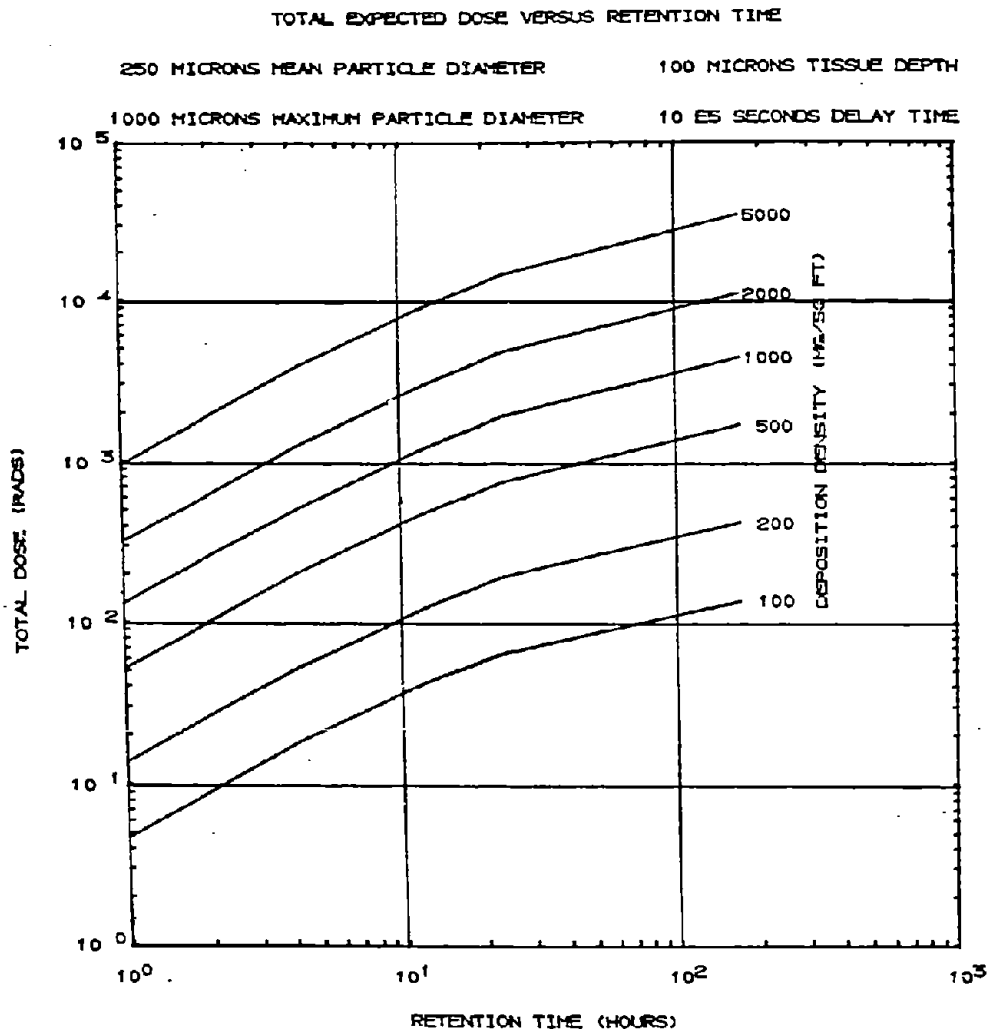


Figure 27
Beta Dose Delivered to the
Skin by Multiparticle Fallout

TOTAL EXPECTED DOSE VERSUS RETENTION TIME

500 MICRONS MEAN PARTICLE DIAMETER

100 MICRONS TISSUE DEPTH

1000 MICRONS MAXIMUM PARTICLE DIAMETER

10¹⁵ SECONDS DELAY TIME

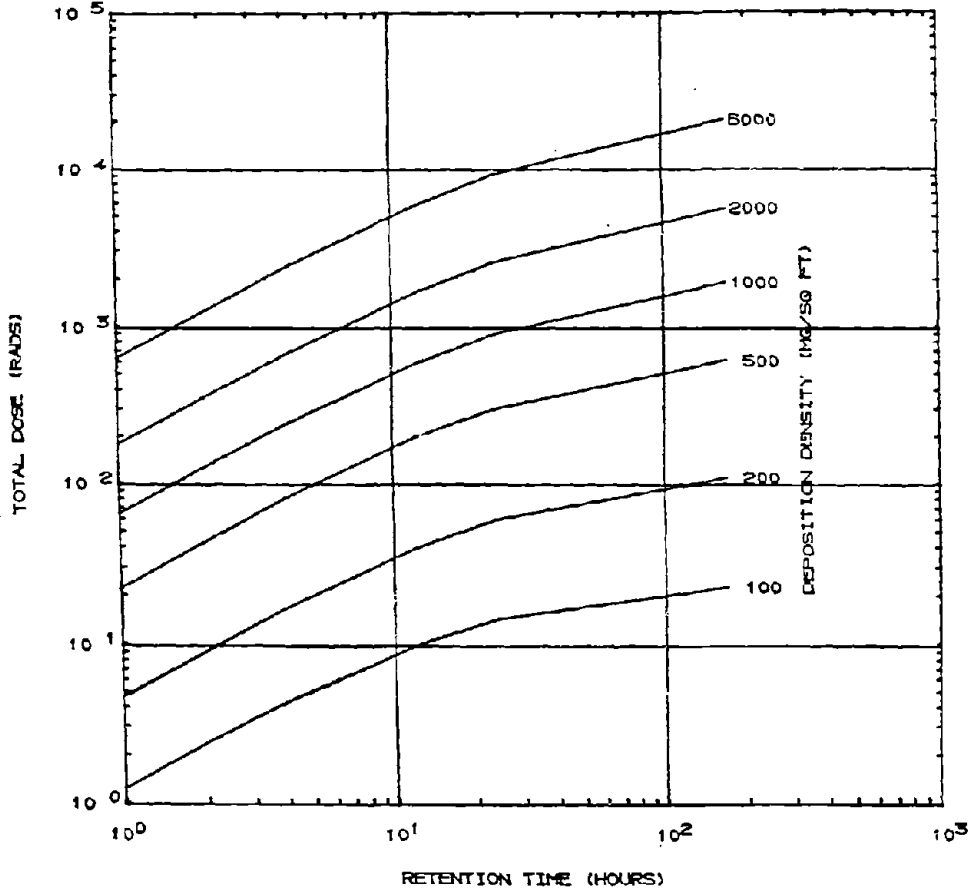


Figure 28

Beta Dose Delivered to the Skin by Multiparticle Fallout

TOTAL EXPECTED DOSE VERSUS RETENTION TIME

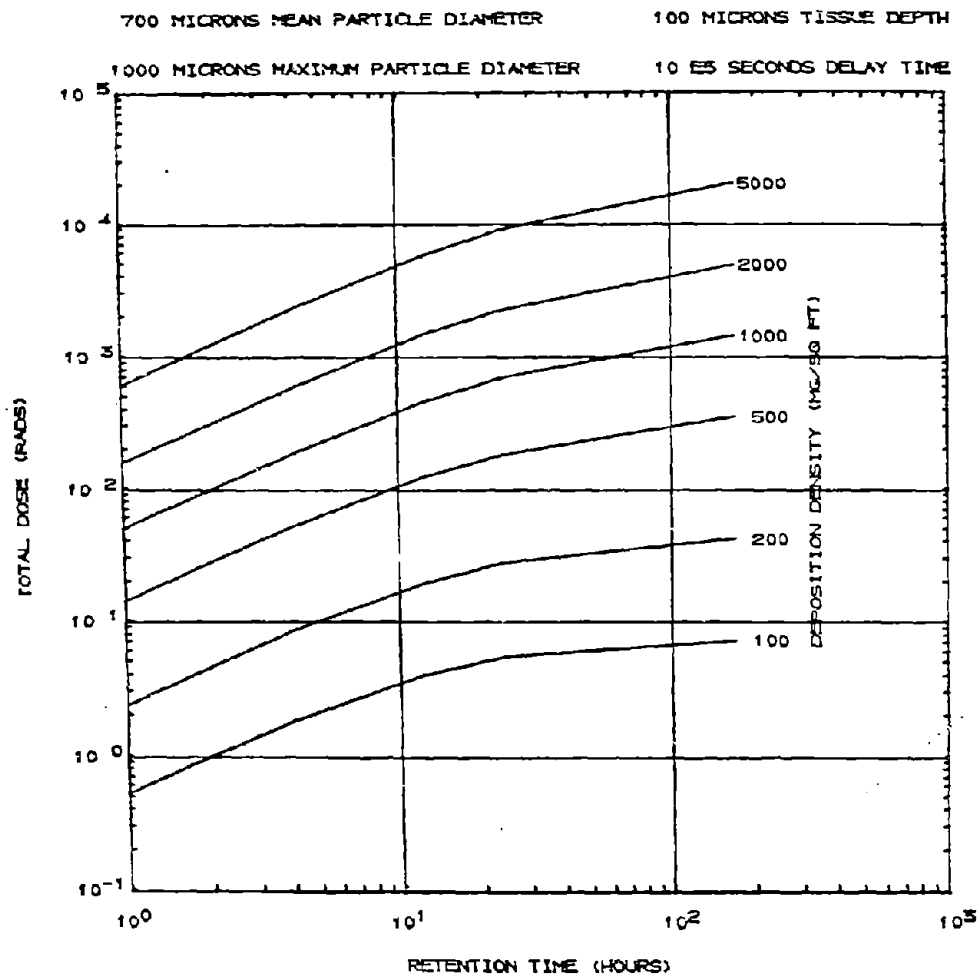


Figure 29

Beta Dose Delivered to the
Skin by Multiparticle Fallout

TOTAL EXPECTED DOSE VERSUS RETENTION TIME

1000 MICRONS MEAN PARTICLE DIAMETER 100 MICRONS TISSUE DEPTH

2000 MICRONS MAXIMUM PARTICLE DIAMETER 10¹⁵ SECONDS DELAY TIME

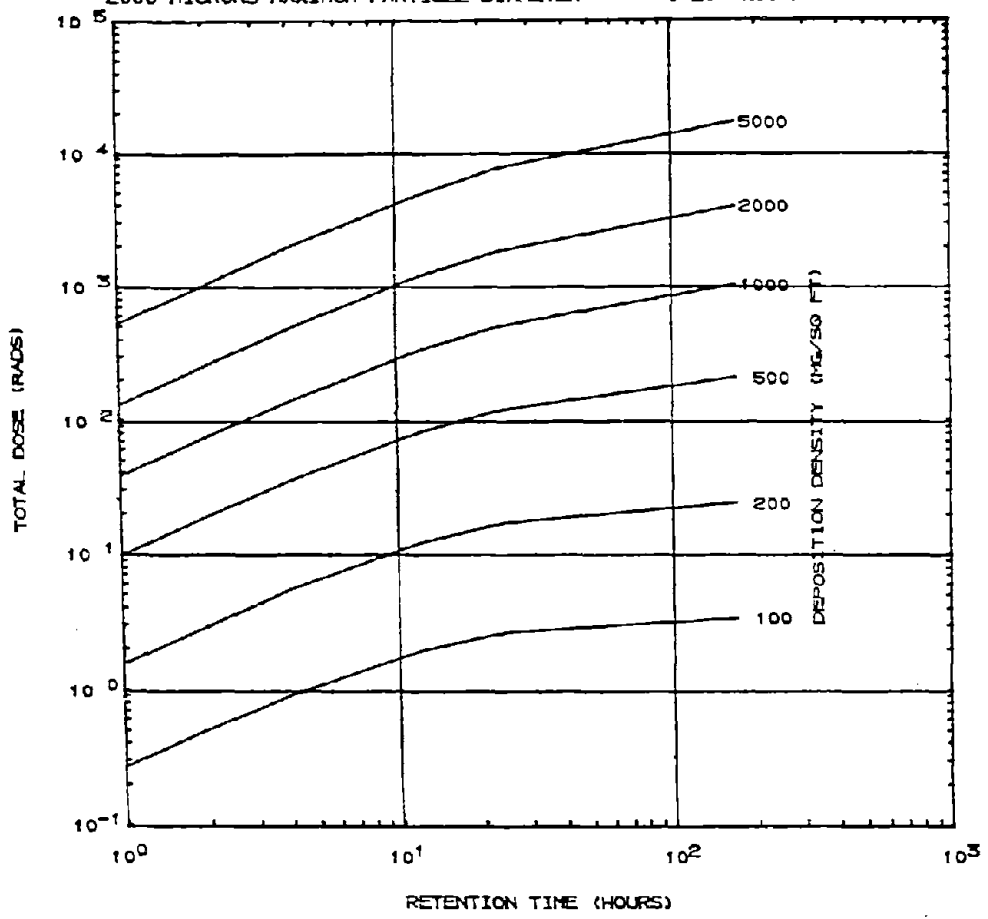


Figure 30

Beta Dose Delivered to the Skin by Multiparticle Fallout

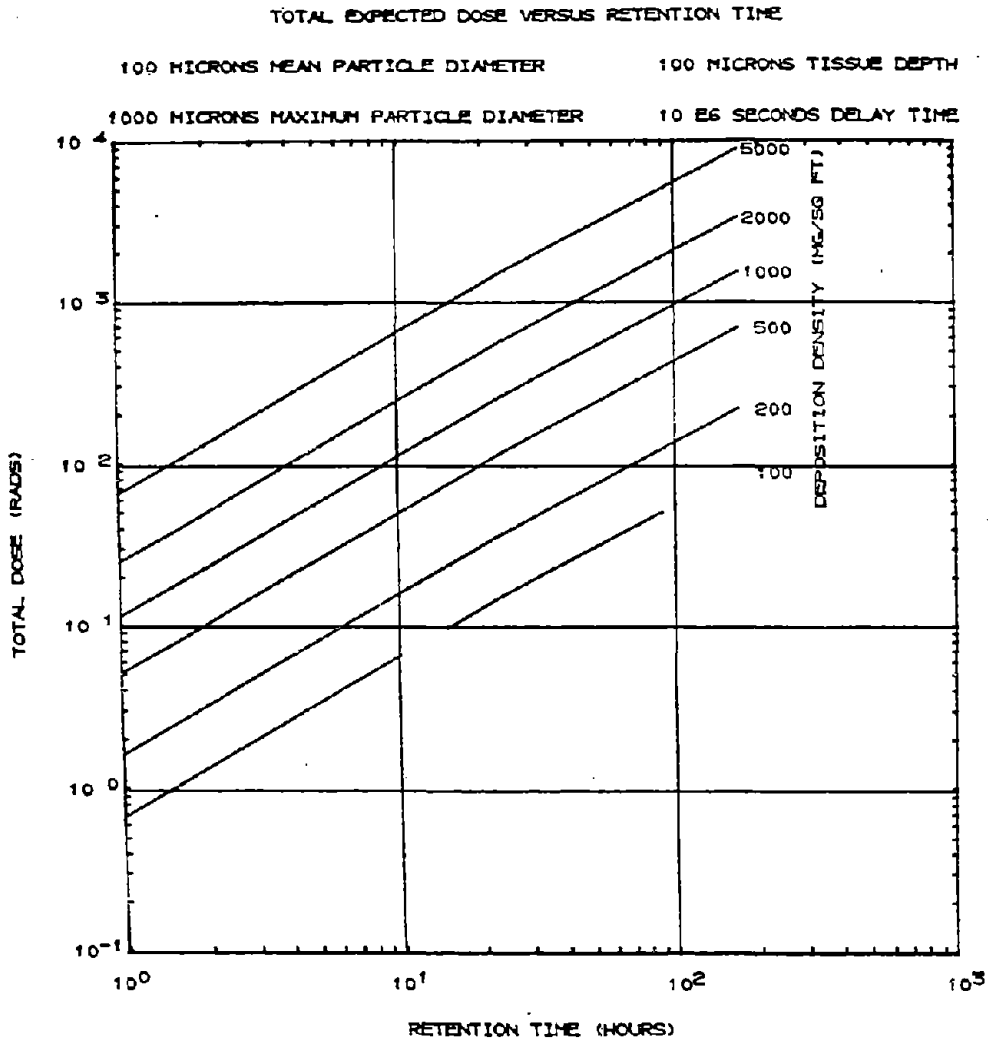


Figure 31
Beta Dose Delivered to the
Skin by Multiparticle Fallout

TOTAL EXPECTED DOSE VERSUS RETENTION TIME

250 MICRONS MEAN PARTICLE DIAMETER

100 MICRONS TISSUE DEPTH

1000 MICRONS MAXIMUM PARTICLE DIAMETER

10¹⁶ SECONDS DELAY TIME

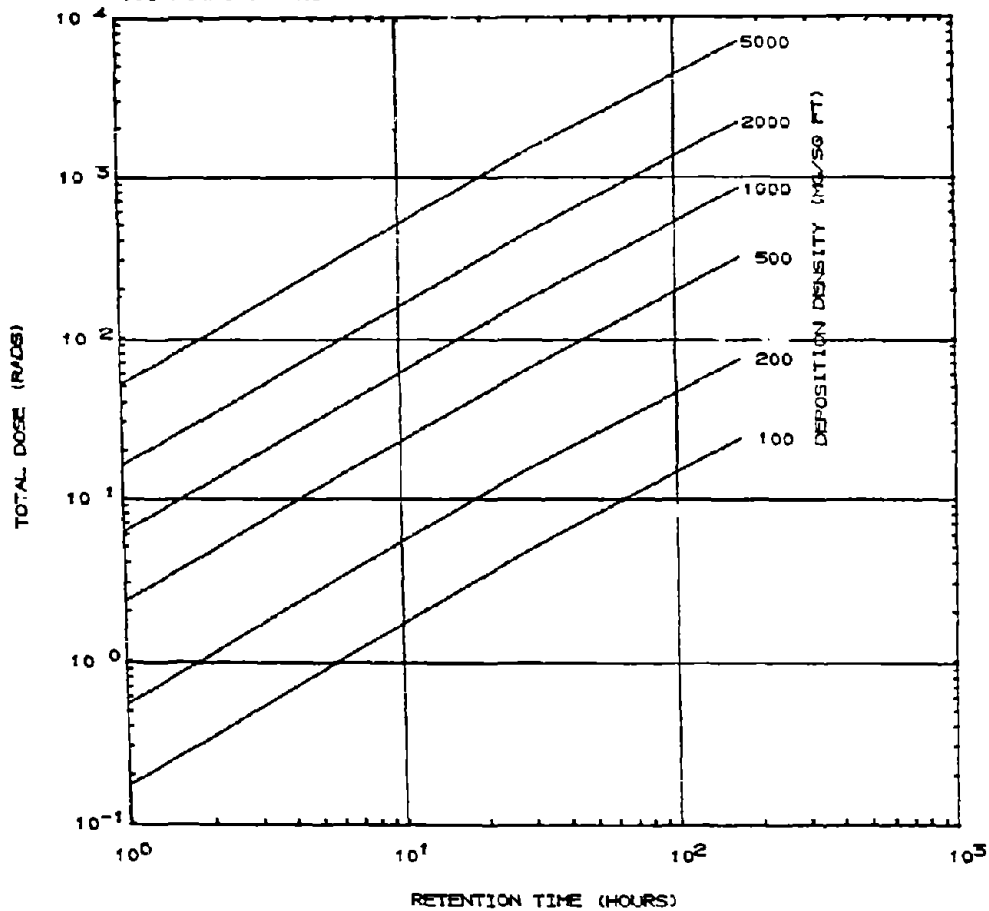


Figure 32

Beta Dose Delivered to the
Skin by Multiparticle Fallout

TOTAL EXPECTED DOSE VERSUS RETENTION TIME

500 MICRONS MEAN PARTICLE DIAMETER

100 MICRONS TISSUE DEPTH

1000 MICRONS MAXIMUM PARTICLE DIAMETER

10 E6 SECONDS DELAY TIME

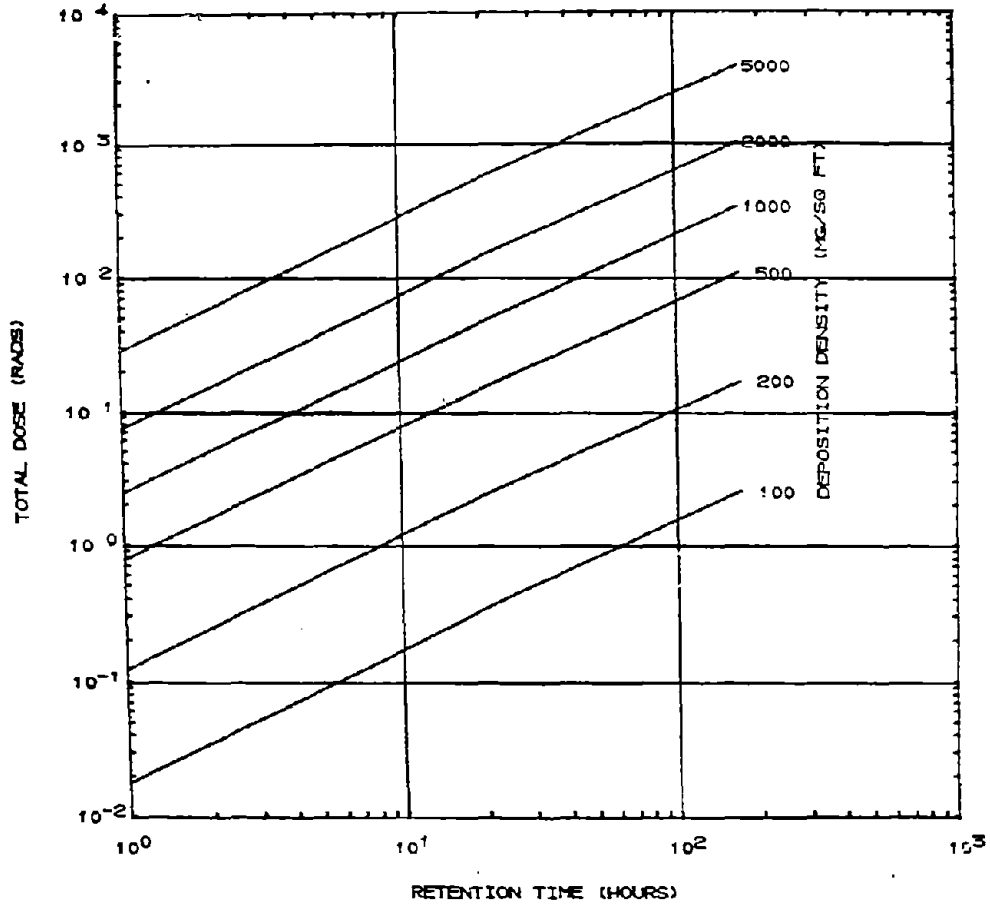


Figure 33

Beta Dose Delivered to the
Skin by Multiparticle Fallout

TOTAL EXPECTED DOSE VERSUS RETENTION TIME

700 MICRONS MEAN PARTICLE DIAMETER

100 MICRONS TISSUE DEPTH

1000 MICRONS MAXIMUM PARTICLE DIAMETER

10 E6 SECONDS DELAY TIME

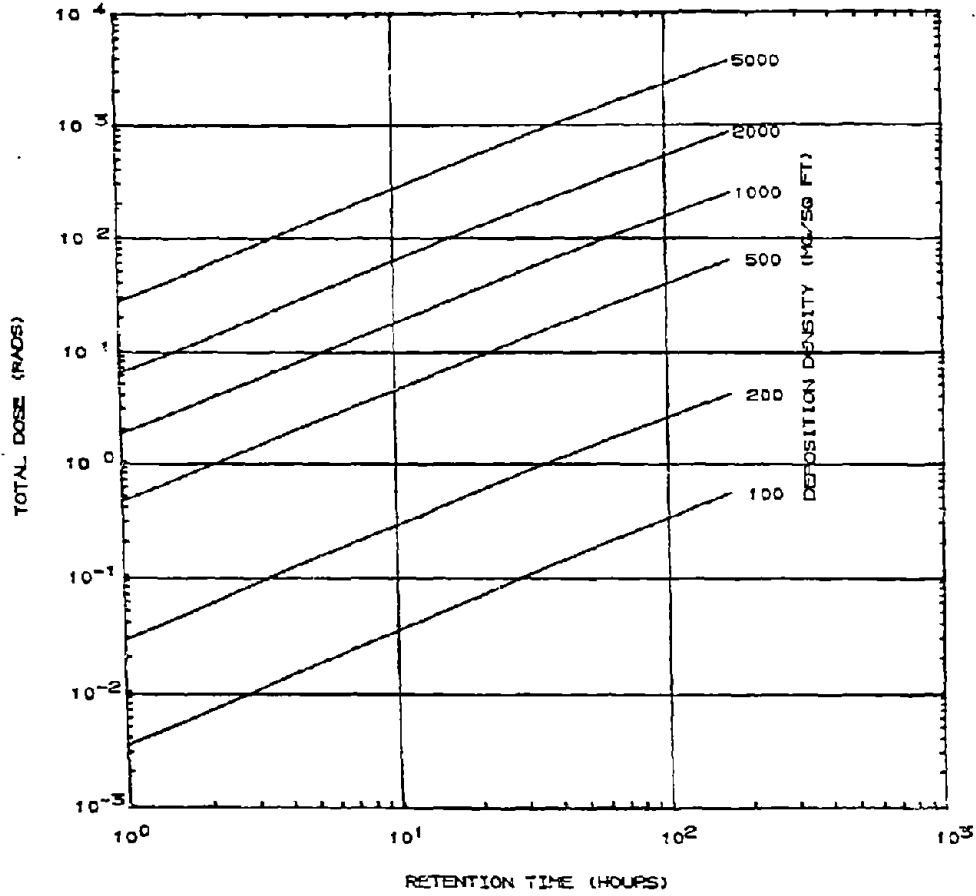


Figure 34

Beta Dose Delivered to the
Skin by Multiparticle Fallout

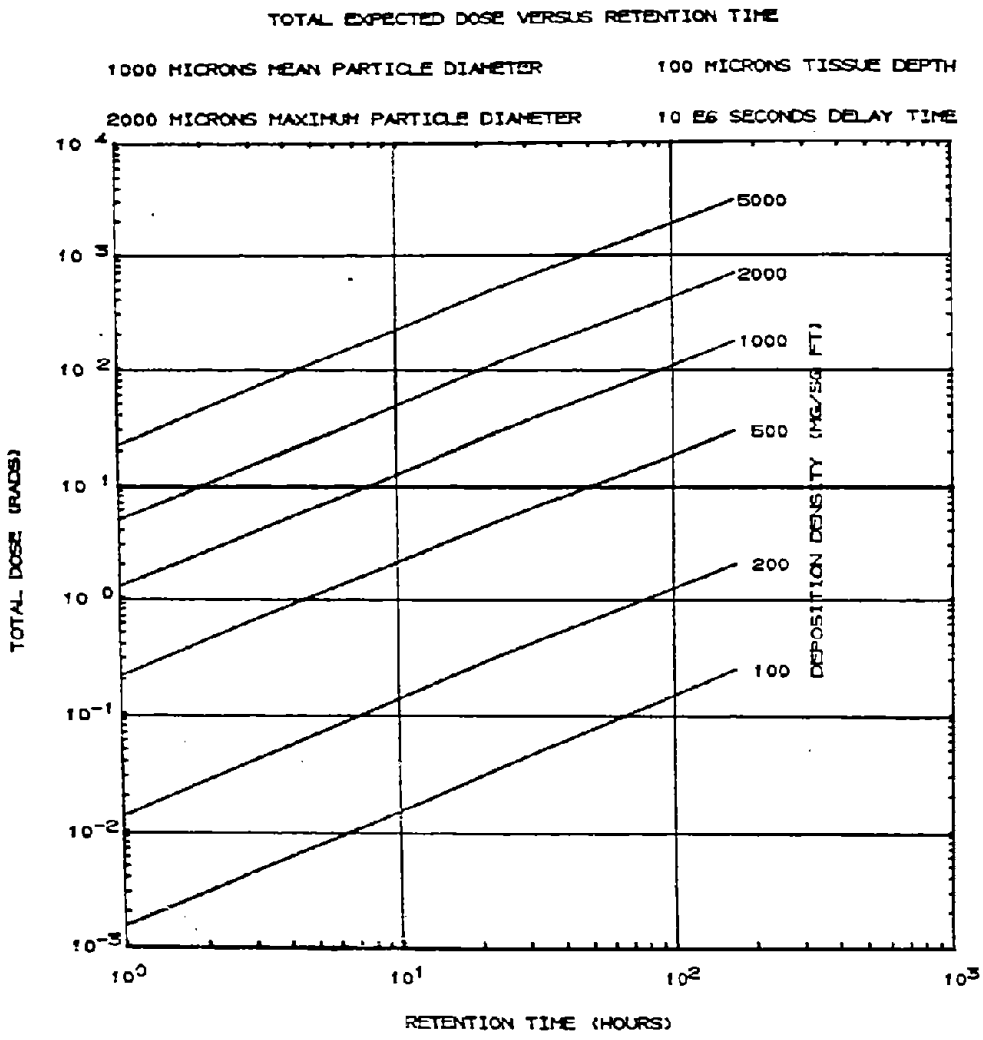


Figure 35
Beta Dose Delivered to the
Skin by Multiparticle Fallout

TOTAL EXPECTED DOSE VERSUS RETENTION TIME

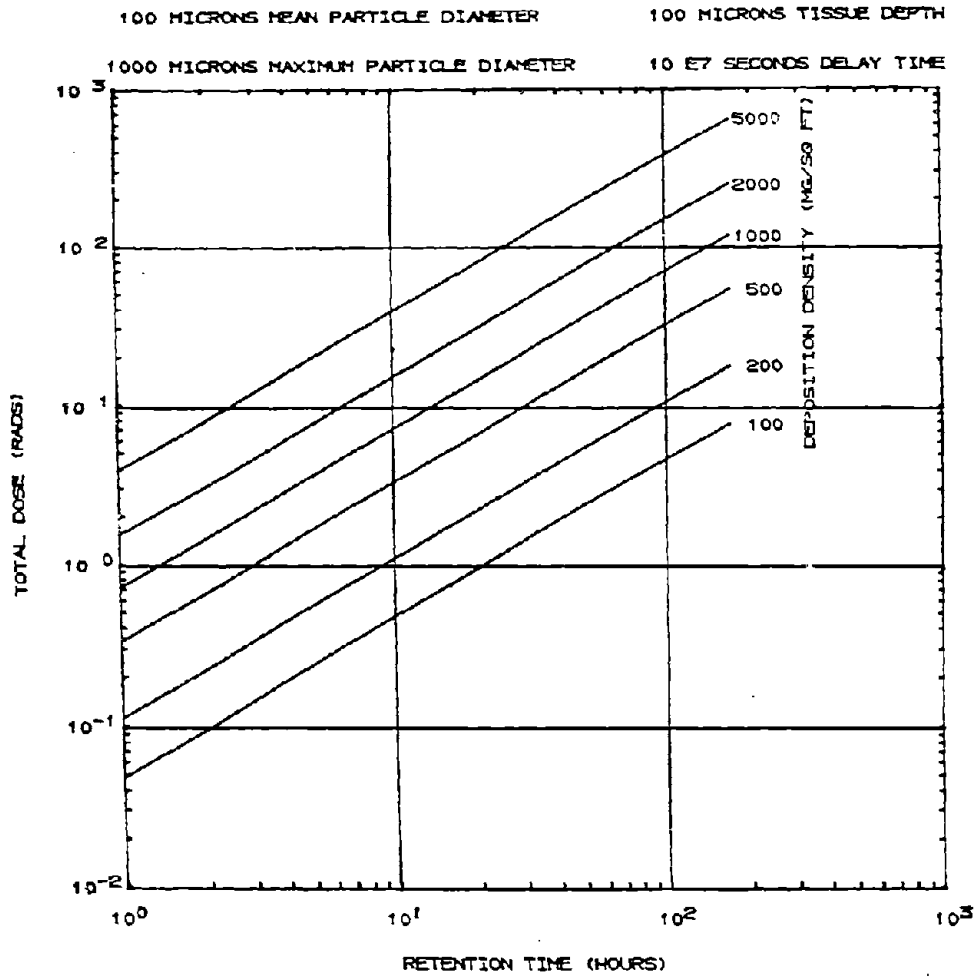


Figure 36
Beta Dose Delivered to the
Skin by Multiparticle Fallout

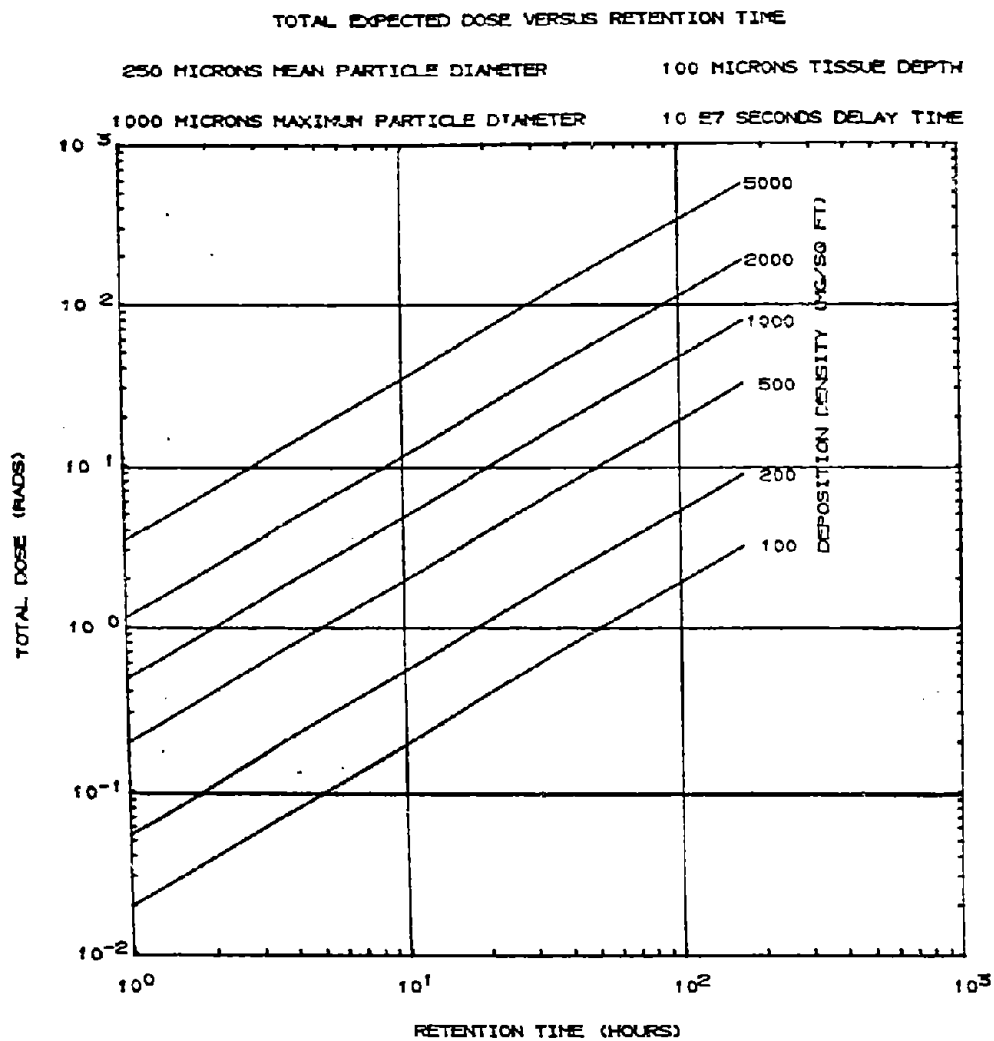


Figure 37
Beta Dose Delivered to the
Skin by Multiparticle Fallout

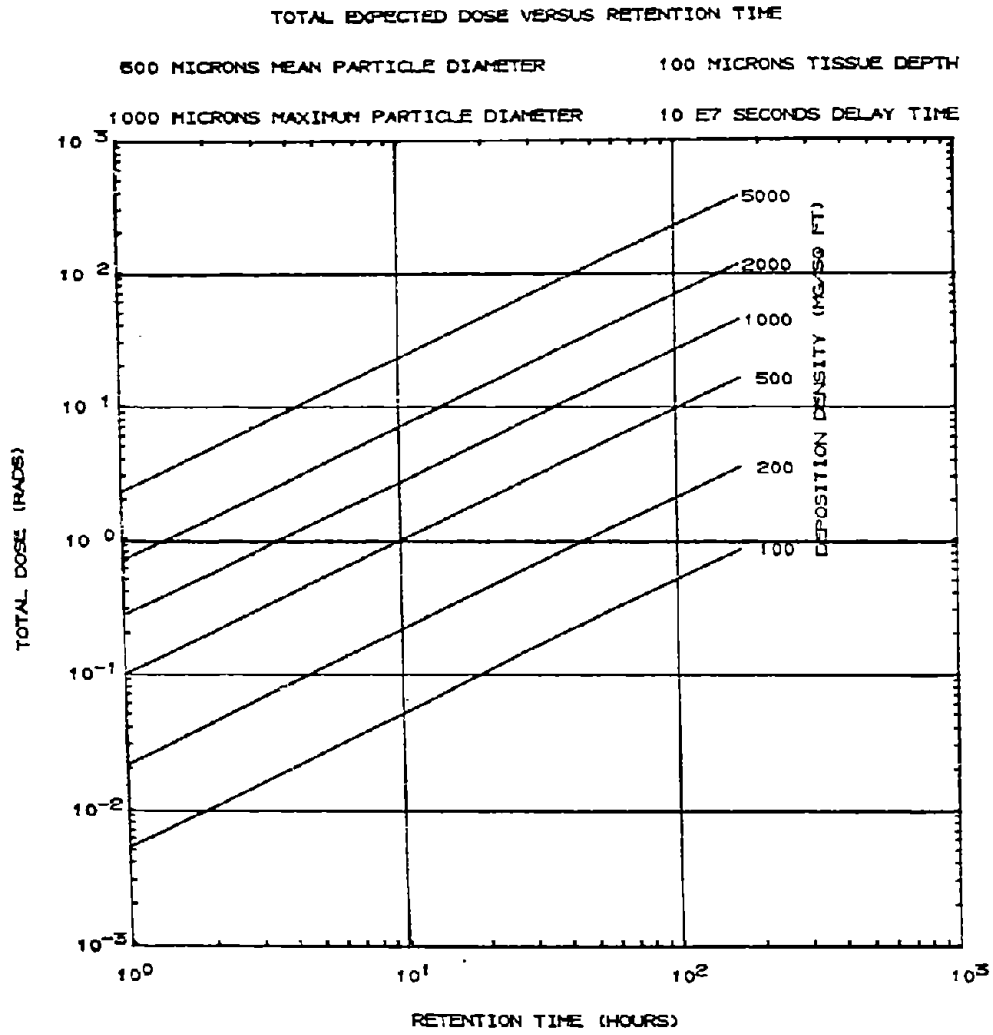


Figure 38
Beta Dose Delivered to the
Skin by Multiparticle Fallout

TOTAL EXPECTED DOSE VERSUS RETENTION TIME

700 MICRONS MEAN PARTICLE DIAMETER

100 MICRONS TISSUE DEPTH

1000 MICRONS MAXIMUM PARTICLE DIAMETER

10 E7 SECONDS DELAY TIME

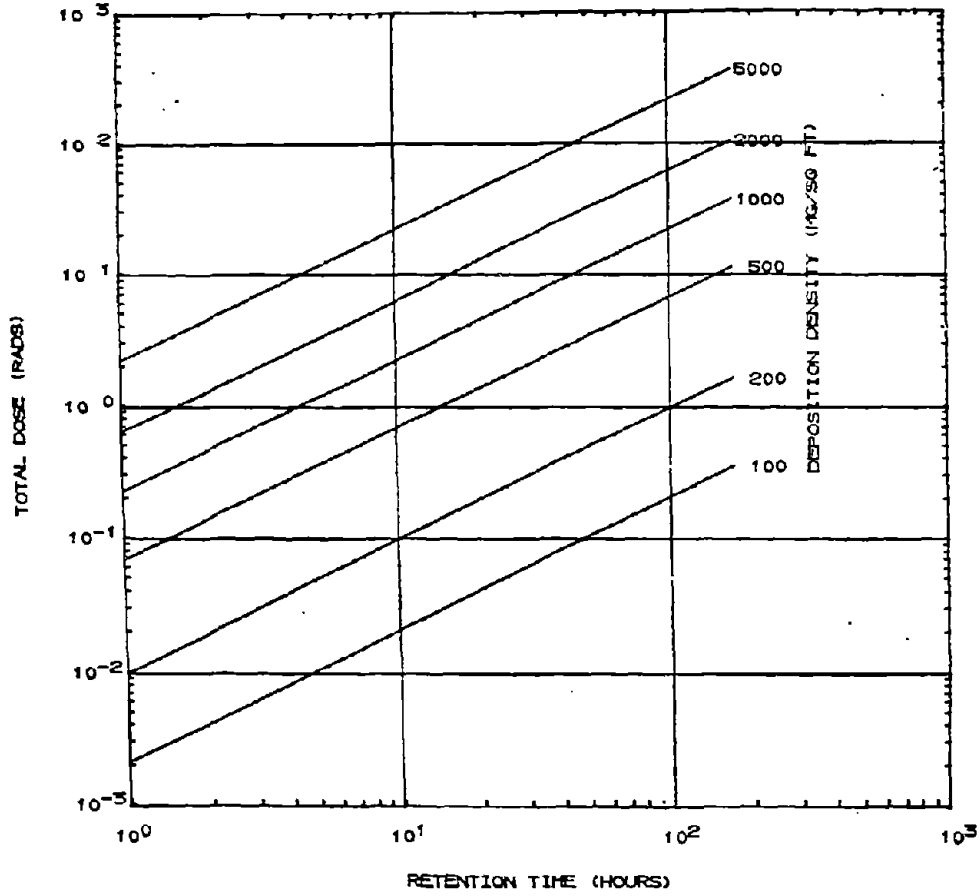


Figure 39

Beta Dose Delivered to the
Skin by Multiparticle Fallout

TOTAL EXPECTED DOSE VERSUS RETENTION TIME

1000 MICRONS MEAN PARTICLE DIAMETER 100 MICRONS TISSUE DEPTH
 2000 MICRONS MAXIMUM PARTICLE DIAMETER 10 E7 SECONDS DELAY TIME

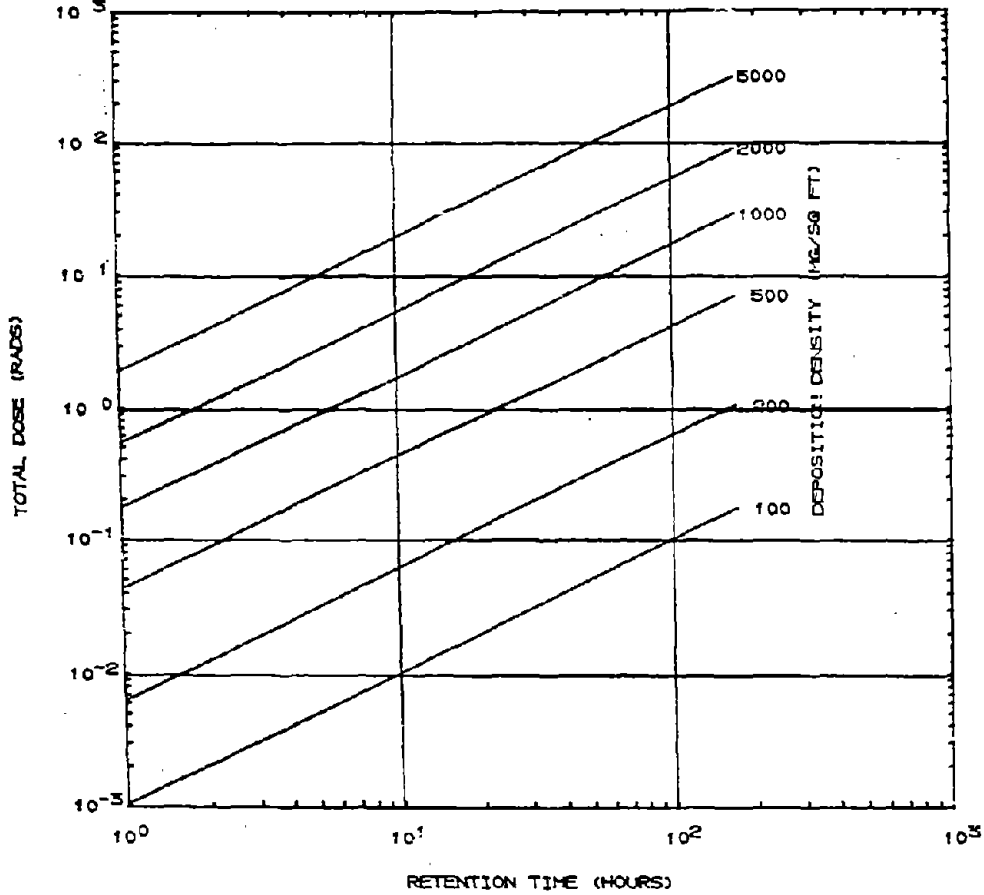


Figure 40

Beta Dose Delivered to the
 Skin by Multiparticle Fallout

(size distribution B) delivers a maximum of 300 rads only, even if retained over 100 hours. Other size distributions give intermediate doses.

The situation changes somewhat at the next higher fall-out-arrival (delay) time, 10^4 seconds. A 200 mg/ft^2 deposit of size distribution A can be tolerated in this case for about 1.5 hours (Figure 21).

After a delay of 10^5 seconds, a 2000 mg/ft^2 deposit of size distribution A gives the critical 570 rads in about 1.5 hours (Figure 26); after a delay of 10^6 seconds (11.5 days) it takes 5000 mg/ft^2 of the same size distribution about ten hours to cause skin burns (Figure 31). By 10^7 seconds it becomes virtually impossible to cause skin damage (Figure 36).

Other formulations of output data can be derived from the multiparticle dose computations. A few examples follow:

Table 10 presents one formulation, the effect of exposure-initiation time (delay time) on the "Krebs" dose received by the skin from the same fallout deposition density. The Table presents doses delivered by two deposition densities, 100 and 2000 mg/ft^2 , in each case over 1, 2, 5, 10 and 24-hour exposure periods, all following delays of 24, 48, 72 and 168 hours. Given also are the time periods for which fallout under these conditions would have to be retained before delivery of 570 rads takes place if the exposure starts at 24, 48, 72 and 168 hours post-detonation. In both parts of the Table, size-distribution A is assumed.

Another type of output formulation that may be useful (not illustrated) would show the skin dose accumulated in one hour (as an example), starting at fallout arrival or some later time, as a function of distance from ground zero, for various

TABLE 10
EFFECT OF EXPOSURE-INITIATION TIME ON KREBS
DOSES DELIVERED TO THE SKIN

Mean Particle Diameter: 100 μ
 Maximum Particle Diameter: 1000 μ

A. Fallout Deposition Density: 100 mg/ft²
 (= 4 x 10¹³ fissions/ft²)

1. Doses Received

Retention Time (hours)	Exposure-Initiation Time			
	24h	48h	72h	168h
1	18 Rad	8 Rad	5 Rad	2 Rad
2	36	16	10	4
5	84	39	24	9
10	151	73	46	17
24	291	153	101	41

2. Retention Times Required to Accumulate 570 Rads

76 hours	250 hours	600 hours	2400 hours
----------	-----------	-----------	------------

TABLE 10 (Cont'd)

B. Fallout Deposition Density: 2000 mg/ft^2
 (= 8×10^{14} fissions/ft²)

1. Doses Received

Retention Time (hours)	Exposure-Initiation Time			
	24h	48h	72h	168h
1	466 Rads	217 Rads	120 Rads	50 Rads
2	912	423	230	98
5	2138	998	608	228
10	3862	1879	1182	445
24	7420	3918	2571	1030

2. Retention Times Required to Accumulate 570 Rads

78 min.	170 min.	4h 40 min.	13h 20 min.
---------	----------	------------	-------------

weapon yields. The figure could be obtained by combining the dose data of this report with the data of Clark and Cobbin⁽²²⁾ for example, the latter relating mid-range particle size to downwind distance from ground zero, for different weapon yields. It must be recognized that for a given weapon yield and downwind distance, fallout phenomenology, as exemplified by the Clark and Cobbin approach, specifies uniquely not only (1) the mid-range particle size, but also (2) the ground-surface deposition density and (3) the times of fallout arrival and cessation. The unique values of the deposition density and times of arrival and cessation would have to be considered in the preparation of a family of curves covering a range of weapon yields. Skin deposition density could be parameterized at, for example, 100 mg/ft², which would allow for consideration of fallout-particle resuspension, or simply for normalization to the correct skin-deposition value at each point. A carefully planned family of curves could thus provide a picture of those yields and downwind distances at which a 1-hour exposure to fallout which starts to deposit on the skin at arrival time, or later, would produce the critical skin dose of 570 rad. Such kinds of results could be most useful in post-attack planning.

I. CONCLUSIONS AND RECOMMENDATIONS

In this report the consequences of deposition of fallout particles on human skin are evaluated. The calculations are based on dose-effects criteria provided by prior experimental work on the effect of skin exposure to particulate sources of beta rays.

1. For a single-particle source a beta dose of 660 rads received at points on an equi-dose circle, 4000μ (4 mm) in radius and 100μ below the skin surface, causes a 1 mm diameter ulcer. This ulcer size, small enough to be considered a threshold indicator, yet large enough to be easily observable, is therefore taken as the "threshold" for "noticeable" skin damage. For a multiparticle source, with overlapping radiation fields, the equivalent effect is produced by a uniform dose field of 570 rads at the germinal-layer level (100μ deep in tissue).

2. On the basis of (1) the criterion that 660 rads constitute the threshold for producing noticeable local damage to the skin (beta burn), and (2) the assumption that fallout has a fission density of 10^{15} fissions per cubic centimeter, it is not expected that single fallout particles less than 500μ in diameter would deliver sufficient beta dose to cause such damage even if they deposit on the skin as early as 10^3 seconds (16.7 minutes) after detonation. The corresponding minimum delay in arrival for a 750μ particle is about two hours, while for a 1000μ particle it is about three hours. These time estimates are based on experimentally determined "expected" particle residence times on the skin. However, after a 24-hour arrival delay it is extremely unlikely that any single particle will

cause a beta burn, even for particle residence times far greater than the expected values.

3. A group of particles deposited on the skin, but separated in geometry such that their dose deliveries at any point in the plane of the germinal layer do not interact appreciably, can be viewed as a collection of independent single particles. On the other hand, multiple-particle deposition denotes a situation in which particles are sufficiently close so that their collective dose delivery at any particular point in the germinal layer is appreciably higher than that, at the same point, from any one particle.

4. In local fallout, fractionation causes a decrease in particle dose delivery. Particles of the same size, containing fission products resulting from the same number of equivalent fissions (estimated from their content of refractory fission products), may deliver beta doses over a range of a factor of 2, the differences depending on the degree of fractionation of their fission-product mixtures.

5. Based on limited calculations (for 100 μ -diameter particles only), it was concluded that gamma doses from fallout particles constitute a small fraction (about 5% in the cases considered) of the total dose delivered by the particles to the skin. For larger particles, the γ -to- β dose ratios are expected to be higher. More work is needed, however, if quantitative values of the dose ratios are desired for the whole spectrum of fallout-particle size.

6. Multiparticle deposition can be represented by two models: (1) a simple, but gross, model in which the radioactive source is treated as a uniform plane source; and (2) a more realistic model in which the source retains its particulate

configuration but the geometry is idealized into an overlay (superimposed) structure of arrays. Each array is composed of equal-size fallout particles located at the corners of square unit-cells, whose dimensions depend on the fallout deposition density for the particle-size class in question. All multiparticle source calculations in this report were based on the more realistic particle-array model. Some dose comparisons were made with sample results based on the uniform-plane-source model.

7. For the same fallout deposition density, the plane-source model yielded dose values higher by a minimum of 400% than those from the particulate (array) model. The discrepancy becomes greater as the mean fallout-particle size becomes larger.

8. Based on the results of the particulate (array) model, the main determinations and conclusions regarding skin exposure to multiparticle fallout can be summarized as follows:

a. Because skin beta doses from fallout are functions of several parameters or conditions, including weapon type, weapon yield, fission density, particle-size distribution, type of soil on which the weapon is detonated, delay time, skin deposition density, and atmospheric conditions (which affect particle residence time on the skin), it was obviously not possible to calculate the doses for all possible combinations of these parameters or conditions and to obtain, as one ideally should, an envelope of situations under which fallout beta dose represents a threat. Rather, calculations were carried out for a representative number of cases chosen to sample as much of the overall spectrum of situations as possible.

b. Dose delivery is strongly affected by the size distribution of the particles. For example, on the assumption

that fallout (of all particle sizes) remains on the skin for 10 hours, the calculations show that a 1 gm/ft² deposit in which the mean particle diameter is 100 μ and the maximum is 1000 μ would cause beta burns even if the fallout arrives as late as 3 days after detonation*. However, if the mean particle size is 1000 μ and the maximum is 2000 μ , the same deposit would be incapable of producing a beta burn if it settles on the skin later than about 17 hours post detonation. Intermediate size distributions have limiting arrival times between these two extremes.

c. A similar subset of values can be obtained for other deposition densities. Further, if any assumption concerning the fallout activity, deposition density or residence time is changed, a totally new set of arrival times is obtained.

The main point that should be made here is that the parametric approach followed in this report provides a numerical base that can, with a little manipulation, supply the user with the answers he needs if he is willing to state a particular set of assumptions that would be acceptable to him and adequate for his purpose.

9. Several of the existing fallout models supply unique combinations of values for fallout arrival time, deposition density, particle-size distribution, and specific activity (fission density). These values can be used as inputs to the single-or multiple-particle beta-dose models (as the situation may demand) to predict beta-dose contours. Such contours should be helpful in casualty assessment and post-attack planning. It is recommended that such a program be undertaken.

*There is no implication here that this would be a realistic combination of parameters.

10. It is recommended also that studies be initiated to answer the following questions and others in the same category of interest to civil defense planning:

a. Is it possible to produce beta burns in the feet, through standing or walking in a contaminated area, under conditions where the whole-body gamma dose would not be significant?

b. If the answer to a. is positive, under what circumstances would the beta exposure be the limiting factor?

c. What are the expected beta-dose deliveries to cattle and sheep? Can these predicted doses be coupled to the results of the ongoing OCD-sponsored experimental work on beta effects on animals, to yield cattle- and sheep-casualty assessments?

It is felt that the true value of the experimental work on the effects of beta exposure on plants and animals cannot be realized unless it leads to credible evaluations of the expected losses in the U. S. inventory of these important resources in the immediate post-attack era. It is believed that the multi-particle TDD model can supply the required linkage between experimental biology and fallout models, the combination of which is mandatory for plausible casualty appraisals. Confirmation of the validity of the TDD model predictions by the experimental (physics) program described in an early section of this report provides a firm basis for confidence in the calculational approach.

XI. REFERENCES

1. R. Loevinger, E. M. Japha, and G. C. Brownell, Discrete Radioisotope Sources, in Radiation Dosimetry, Hine and Brownell, Eds., pp. 693-754, Academic Press, Inc. New York, 1956.
2. J. C. Ulberg and D. B. Kochendorfer, Models for Estimating Beta Dose to Tissue from Particle Debris in Aerospace Nuclear Applications, U. S. Naval Radiological Defense Laboratory Report USNRDL-TR-1107, 1966.
3. O. L. Hogan, P. E. Zigman and J. L. Mackin, Beta Spectra II. Spectra of Individual Negatron Emitters, U. S. Naval Radiological Defense Laboratory Report, USNRDL-TR-802, 1964.
4. C. F. Miller, Fallout and Radiological Countermeasures, Stanford Research Institute Report, SRI Project No. IM-4021, 1963.
5. R. F. Korts and J. H. Norman, A Computational Model for Condensed State Diffusion Controlled Fission Product Absorption During Fallout Formation, General Atomic Report GA-7598, OCD Work Unit No. 3111A, 1967.
6. L. V. Spencer, Energy Dissipation by Fast Electrons, National Bureau of Standards Monograph 1, 1959.
7. G. B. Curtis and J. S. Petty, A Program to Compute Beta Radiation Dosage, American Research Corporation Report ARC 67-48, 1967.
8. S. Z. Mikhail, Tissue Beta Radiation Doses from Particulate Fission Product Sources: Comparison of Model Predictions with Experimental and Monte Carlo Values, Environmental Science Associates Report ESA-TR-70-01, 1970.
9. R. Loevinger, Extrapolation Chamber for the Measurement of Beta Sources, Rev. Sci. Instr., 24: 907 (1953).

10. E. C. Freiling et al., Fractionation IV. Illustrative Calculations of The Effect of Radionuclide Fractionation on Exposure-Dose Rate from Local Fallout, U. S. Naval Radiological Defense Laboratory Report, USNRDL-TR-715, 1964.
11. R. C. Bolles and N. E. Ballou, Calculated Activities and Abundances of ^{235}U Fission Products, U. S. Naval Radiological Defense Laboratory Report, USNRDL-456, 1956.
12. R. D. Present, Phys. Rev., 72:7 (1947)
13. L. E. Glendenin et al., National Nuclear Energy Series, Division 4, 9. McGraw-Hill, 1951. Also, L. E. Glendenin, Massachusetts Institute of Technology, Technical Report No. 35, 1949.
14. E. C. Freiling, Fractionation I. High Yield Surface Burst Correlations, U. S. Naval Radiological Defense Laboratory Report, USNRDL-TR-385, 1959. Also, Science 133:1991 (1961)
15. G. W. Gradstein, X-ray Attenuation Coefficients from 10 Kev to 100 Mev, National Bureau of Standards, Circular 583, 1967.
16. H. Goldstein, The Attenuation of Gamma Rays and Neutrons in Reactor Shields, Division of Reactor Development, USAEC, 1957.
17. J. S. Krebs, The Response of Mammalian Skin to Irradiation with Particles of Reactor Debris, U. S. Naval Radiological Defense Laboratory Report, USNRDL-TR-67-118, 1967.
18. P. D. Forbes and S. Z. Mikhail, Acute Lesions in Skin Produced by Radioactive Microspheres, Temple University Report, Contract SNPN-49, 1970.

19. S. L. Brown, Disintegration Rate Multipliers in Beta-Emitter Dose Calculations, Stanford Research Institute Report, SRI Project MU-5116, 1965.
20. J. S. Krebs, personal communication, September 1970.
21. B. R. Fish, et al., Environmental Studies: Radiological Significance of Nuclear Rocket Debris, Progress Report 1 July - 31 December, 1964(U), Oak Ridge National Laboratory Report ORNL-TM-1053, 1965 (Classified).
22. D. E. Clark, Jr. and W. C. Cobbin, Some Relationships Among Particle Size, Mass Level and Radiation Intensity of Fallout from A Land Surface Nuclear Detonation, U. S. Naval Radiological Defense Laboratory Report, USNRDL-TR-639, 1963.

DISTRIBUTION LIST

(One copy to each addressee unless otherwise indicated.)

Office of the Secretary of the
Army
Office of Civil Defense
Research
Pentagon
Washington, D. C. 20310
Attn: Administrative Officer
(40)

Army Library
1A518, Pentagon
Washington, D. C. 20310

Assistant Secretary of the Army
(R&D)
Washington, D. C. 20310
Attn: Assistant for Research

Chief of Naval Research
Washington, D. C. 20360

Commander
Naval Supply Systems Command
(Code 0611C1)
Department of the Navy
Washington, D. C. 20360

Commander
Naval Facilities Engineering
Command
Research and Development
(Code 0322C)
Department of the Navy
Washington, D. C. 20390

Defense Documentation Center
Cameron Station
Alexandria, Virginia 22314
(12)

Advisory Committee on Civil Defense
National Academy of Sciences
2101 Constitution Avenue, N. W.
Washington, D. C. 20418
Attn: Mr. Richard Park

Civil Defense Research Project
Oak Ridge National Laboratory
P. O. Box X
Oak Ridge, Tennessee 37830
Attn: Librarian

Chief
Joint Civil Defense Support Group
Office of Chief of Engineers
Department of the Army
Forestal Building, 1F035
Washington, D. C. 20314

Chief
Engineer Strategic Studies Group
Office of Chief of Engineers
6500 Brooks Lane, N. W.
Washington, D. C. 20315

Ballistic Research Laboratory
Aberdeen Proving Ground,
Maryland 21005
Attn: Librarian

Technical Library
USA-MERDC
Building 315
Fort Belvoir, Virginia 22060

Defense Atomic Support Agency
Washington, D. C. 20305
Attn: Librarian

National War College
Fort Leslie J. McNair
Washington, D. C. 20315
Attn: Librarian

Dr. Carl F. Miller
Dikewood Corporation
1009 Bradbury Drive, S. E.
University Research Park
Albuquerque, New Mexico 87106

Commander, NMCSSC
Pentagon, Room BE-685
Washington, D. C. 20310

Dr. Abner Sachs
Institute for Defense Analysis
400 Army Navy Drive
Arlington, Virginia 22202

Defense Intelligence Agency
Arlington Hall Station
B. Bldg. Room 0100
Arlington Hall
Arlington, Virginia 22212
Attn: DS-4A

Mr. Burke Stannard
Defence Research Board
Defence Research Analysis Establishment
National Defence Headquarters
Ottawa 4, Ontario, Canada

Dr. Harold Knapp
Weapons Systems Evaluation Group
400 Army Navy Drive
Arlington, Virginia 22202

Mr. Edward Saunders
Office of Emergency Preparedness
17th & F. Streets, N. W.
Washington, D. C. 20504

Defense Atomic Support Agency
Commander Field Command
Sandia Base
Albuquerque, New Mexico 87115

Mr. William White
Stanford Research Institute
Menlo Park, California 94025

U. S. Atomic Energy Commission
Headquarters Library, G049
Washington, D. C. 20545

Dr. Eugene Wigner
Civil Defense Research Project
Oak Ridge National Laboratory
Oak Ridge, Tennessee 37831

Director Disaster and Defense
Services Staff
Agricultural Stabilization and
Conservation Service
U. S. Department of Agriculture
Washington, D. C. 20250

Mr. Myron B. Hawkins
URS Research Company
155 Bovet Road
San Mateo, California 94402

Civil Defense Technical Services
Center
College of Engineering
Department of Engineering
Gainesville, Florida 32601

Dr. Bernard Shore
University of California
Lawrence Radiation Laboratory
P. O. Box 808
Livermore, California 94550

Mr. Joseph Maloney
Ballistic Research Laboratories
Aberdeen Proving Ground,
Maryland 21005

Dr. E. C. Sharman
Agricultural Research Service
U. S. Department of Agriculture
307A Administration Building
Washington, D. C. 20250

Defense Atomic Support Agency
2020 - 14th Street
North Arlington, Virginia 22201
Attn: MAJ George Conner

Dr. Arnold H. Sparrow
Biology Department
Brookhaven National Laboratory
Upton, Long Island, New York 11973

U. S. Atomic Energy Commission
Fallout Studies Branch, DBM
Washington, D. C. 20545
Attn: Dr. Rudolf J. Engelmann

U. S. Office of Education
Department of Health, Education and
Welfare
Washington, D. C. 20202
Attn: Director, Civil Defense Adult
Education Staff

U. S. Atomic Energy Commission
Environmental Sciences Branch, DBM
Washington, D. C. 20545
Attn: Dr. Charles Osterberg

Director
Division of Health Mobilization
U. S. Public Health Service
Department of Health, Education and
Welfare
Washington, D. C. 20202

U. S. Atomic Energy Commission
Biological Effects Branch, DBM
Washington, D. C. 20545
Attn: Dr. Robert Rabson

U. S. Atomic Energy Commission
Civil Effects Branch, DBM
Washington, D. C. 20545
Attn: Mr. L. Joe Deal

Mr. Paul Zigman
Environmental Science Associates
770 Airport Boulevard
Burlingame, California 94010
(10)

Dr. J. J. Davis
U. S. Atomic Energy Commission
Nevada Operations Office
Effects Evaluation Division
Las Vegas, Nevada 89100

Dr. William A. Rhoads
EG&G, Inc.
Santa Barbara Division
130 Robin Hill Road
Goleta, California 93017

Mr. George H. Walter
U. S. Department of Agriculture
218-E Administration Building
14th & Independence Ave., S. W.
Washington, D. C. 20250

Dr. John Norman
Gulf Energy and Environmental
Systems, Inc.
P. O. Box 608
San Diego, California 92112

Oak Ridge National Laboratory
Ecological Sciences Division
Bldg. 2001
Oak Ridge, Tennessee 37831
Attn: Dr. Stanley I. Auerbach

Dr. Robert K. Schulz
University of California
Department of Soils and Plant
Nutrition
Berkeley, California 94720

Dr. Lewis V. Spencer
National Bureau of Standards
Radiation Theory Section
Washington, D. C. 20324

Dr. Cyril L. Comar
Cornell University
Department of Physical Biology
Ithaca, New York 14850

Dr. Milton J. Constantin
UT-AEC Agricultural Research
Laboratory
1299 Bethel Valley Road
Oak Ridge, Tennessee 37830

Dr. John R. Rust
University of Chicago
Section of Nuclear Medicine
947 E. 58th Street
Chicago, Illinois 60600

Dr. M. C. Bell
UT-AEC Agricultural Research
Laboratory
1299 Bethel Valley Road
Oak Ridge, Tennessee 37830

Dr. Leo K. Bustad
University of California
Davis, California 95616

Dr. Harold Brode
RAND Corporation
Santa Monica, California 90406

Dr. Vernon M. Stern
University of California
Agricultural Experiment Station
Riverside, California 92502

Mr. Robert M. Rodden
Stanford Research Institute
Menlo Park, California 94025

Mr. William B. Lane
Stanford Research Institute
Menlo Park, California 94025

Dr. Stephen L. Brown
Stanford Research Institute
Menlo Park, California 94025

Dr. Eric Clarke
Technical Operations Research
Burlington, Massachusetts 01338

UNCLASSIFIED

Security Classification

DOCUMENT CONTROL DATA - R & D

(Security classification of title, body of abstract and indexing annotation must be entered when the overall report is classified)

1. ORIGINATING ACTIVITY (Corporate author) Environmental Science Associates 770 Airport Boulevard Burlingame, California 94010		2a. REPORT SECURITY CLASSIFICATION Unclassified	
		2b. GROUP N/A	
3. REPORT TITLE Beta - Radiation Doses from Fallout Particles Deposited on the Skin			
4. DESCRIPTIVE NOTES (Type of report and inclusive dates) Final Report - 17 April 1970 - 30 June 1971			
5. AUTHOR(S) (First name, middle initial, last name) Saad Z. Mikhail			
6. REPORT DATE January 1971	7a. TOTAL NO. OF PAGES 107	7b. NO. OF REFS 22	
8a. CONTRACT OR GRANT NO. Contract No. DAHC20-70-C-0289	8b. ORIGINATOR'S REPORT NUMBER(S) ESA-TR-71-01		
8c. PROJECT NO. OCD Work Unit No. 3117G	8d. OTHER REPORT NO(S) (Any other numbers that may be assigned this report) N/A		
9. DISTRIBUTION STATEMENT Approved for public release; distribution unlimited			
11. SUPPLEMENTARY NOTES None	12. SPONSORING MILITARY ACTIVITY Director of Research Office of Civil Defense, Dept. of the Army Washington, D. C. 20310		
13. ABSTRACT Absorbed beta-radiation dose expected from fallout particles deposited on the skin was estimated by use of the Beta Transmission, Degradation and Dissipation (TDD) model and a Condensed-State Diffusion-Controlled model that describes the mechanism of fission-product absorption in fallout. A fission density of 10^{15} fissions per cubic centimeter of fallout material was assumed. Comparison of computed doses with the most recent experimental data relative to skin response to beta-energy deposition leads to the conclusion that even for fallout arrival times as early as 10^2 seconds (16.7 minutes post-detonation), no skin ulceration is expected from single particles 500 micron or less in diameter. Doses were estimated for a limited number of particulate sources containing fractionated fission-product mixtures. Results indicate that extreme fractionation would cut down the beta dose by a factor of two. Absorbed gamma doses calculated for one particle size (100 μ) show a beta-to-gamma ratio of about 15. Dose ratio for larger particle sizes will be smaller. Doses from arrays of fallout particles of different size distributions were computed, also, for several fallout mass deposition densities; time intervals required to accumulate doses sufficient to initiate skin lesions were calculated. These times depend strongly on the assumed fallout-particle-size distribution. Deposition densities in excess of 100 mg per square foot of the skin will cause beta burns if fallout arrival time is less than about three hours, unless the particles are relatively coarse (mean particle diameter more than 250 μ).			

DD FORM 1473

NOV 66

REPLACES DD FORM 1473, 1 JAN 64, WHICH IS OBSOLETE FOR ARMY USE.

UNCLASSIFIED

Security Classification

14. KEY WORDS	LINK A		LINK B		LINK C	
	ROLE	WT	ROLE	WT	ROLE	WT
Skin irradiation						
Beta radiation						
Fallout particles						
Biological hazard						
Acute response						
Gamma radiation						
Fractionation						

UNCLASSIFIED